



Article

# Silicon Nitride Bearings for Total Joint Arthroplasty

Bryan J. McEntire <sup>1,\*</sup>, Ramaswamy Lakshminarayanan <sup>1</sup>, Darin A. Ray <sup>1</sup>, Ian C. Clarke <sup>2</sup>,  
Leonardo Puppulin <sup>3</sup> and Giuseppe Pezzotti <sup>4</sup>

<sup>1</sup> Amedica Corporation, 1885 West 2100 South, Salt Lake City, UT 84119, USA; narayana108@yahoo.com (R.L.); darinaray@gmail.com (D.R.)

<sup>2</sup> Department of Orthopaedics, Loma Linda University, Loma Linda, CA 92354, USA; ithipgeek15@yahoo.com

<sup>3</sup> Department of Molecular Cell Physiology, Graduate School of Medical Science, Kyoto Prefectural University of Medicine, 465 Kajii-cho, Kawaramachi-Hirokoji, Kamigyo-ku, Kyoto 602-8566, Japan; pampu78@gmail.com

<sup>4</sup> Ceramic Physics Laboratory, Kyoto Institute of Technology, Sakyo-ku, Matsugasaki, Kyoto 606-8126, Japan; pezzotti@kit.ac.jp

\* Correspondence: bmcentire@amedica.com; Tel.: +1-801-839-3504

Academic Editor: Thomas J. Joyce

Received: 8 July 2016; Accepted: 1 October 2016; Published: 18 October 2016

**Abstract:** The articulation performance of silicon nitride against conventional and highly cross-linked polyethylene, as well as for self-mated silicon nitride bearings, was examined in a series of standard hip simulation studies. Wear rates for polyethylene liners against silicon nitride femoral heads were consistent with reported literature, although higher than cobalt chromium controls. Excessive protein precipitation was a confounding factor in interpretation of the wear data. Post wear-test Raman spectroscopy of the cross-linked polyethylene liners showed no oxidative degradation. Wear of self-mated silicon nitride was found to be essentially zero and indistinguishable from alumina controls using continuously orbital hip simulation for up to three million cycles. However, introduction of an alternative loading profile from three to five million cycles, including a *stop-dwell-start* sequence, significantly increased wear for two of six silicon nitride couples. This behavior is associated with formation and disruption of a gelatinous silicic acid tribochemical film, and is consistent with a recurrent transition from fluid-film to boundary lubrication. Overall, these results suggest that silicon nitride articulation against dissimilar counterface surfaces (e.g., highly cross-linked polyethylene) is preferred.

**Keywords:** silicon nitride; friction; wear; hip simulation; polyethylene; tribochemical film

**PACS:** J0101

## 1. Introduction

Since 2008 silicon nitride ( $\text{Si}_3\text{N}_4$ ) has been used as arthrodesis devices in the cervical and thoracolumbar spine [1], and has been proposed as a new bearing material for total joint arthroplasty [2–5].  $\text{Si}_3\text{N}_4$  has a favorable combination of properties, such as high strength and fracture toughness [4], inherent phase stability [4], biocompatibility [6], hydrophilicity [7], and bacterial resistance [7,8], all of which make it ideal for these applications. However, its performance as an arthroplastic bearing has yet to be fully evaluated. Laboratory studies have shown that its friction and wear are critically dependent on applied load, sliding speed, environment, and counterface material [9–26]. In articulation against polyethylene (PE), low friction is typically observed for all ceramics, including various  $\text{Si}_3\text{N}_4$  compositions (i.e.,  $<0.12$ ) [27–31]; and even lower friction (i.e.,  $<0.01$ ) has been reported for  $\text{Si}_3\text{N}_4$  sliding against carbon-fiber reinforced polyetheretherketone (CRF-PEEK) [23]. For self-mated  $\text{Si}_3\text{N}_4$ , extremely low friction ( $\leq 0.002$ ) and wear have been seen under well controlled, low-load, high-speed,

and continuous motion devices; whereas high friction ( $>0.7$ ) and accelerated wear are apparent for slow-speed, high-loads, and interrupted (*stop-start*) conditions [10]. This varied behavior is due to  $\text{Si}_3\text{N}_4$ 's surface chemistry. It is a non-oxide ceramic in its bulk; but it possesses a protective Si-N-O transitional layer at its surface. Tribochemical wear of this layer leads to the release of ammonia ( $\text{NH}_3$ ) and formation of a lubricating fluid film consisting of hydroxylated silicic acid ( $\text{Si}(\text{OH})_4 \cdot x\text{H}_2\text{O}$ ) which flattens asperities, and can lower friction under low-load, continuous motion conditions. The resultant wear products are soluble and resorbable, potentially leading to a reduction in wear-debris induced osteolysis [32–34]. However, inadequate formation of the tribochemical film during high loads or under *stop-start* cycling results in boundary layer lubrication and high friction. Marked changes in load or slight perturbations of the wear track cause dramatic frictional fluctuations leading to *stick-slip* behavior.

In this paper the *in vitro* performance of  $\text{Si}_3\text{N}_4$  total hip arthroplasty (THA) bearings from three separate hip simulator studies are reported. Hip simulator testing is an accepted practice and a regulatory prerequisite for new or novel materials to ascertain whether proposed wear couples increase patient risks or present new worst case conditions prior to their clinical use [35,36]. Two of the hip simulator studies were conducted using  $\text{Si}_3\text{N}_4$  femoral heads articulating against both conventional ultra-high molecular weight polyethylene (UHMWPE) and highly cross-linked polyethylene (XLPE) liners. These tests were performed by separate laboratories using different simulators with cobalt chromium (CoCr) femoral heads as controls. Additionally, a ceramic-on-ceramic (CoC) hip simulator study compared  $\text{Si}_3\text{N}_4$  head and liner pairs to similar components made from  $\text{Al}_2\text{O}_3$ . Collectively, these studies provide both qualitative and quantitative understanding of the potential *in vivo* capability of this biomaterial.

## 2. Materials and Methods

### 2.1. AMTI Ceramic-on-Polyethylene Hip Simulator Study

For this study, acetabular liners ( $\text{Ø}28$  mm ID) were fabricated from conventional GUR 1050 UHMWPE, terminally sterilized using ethylene oxide (EO) and coupled with  $\text{Si}_3\text{N}_4$  ( $\text{MC}^{\text{®}}$ , Amedica, Salt Lake City, UT, USA) [37] or CoCr (ASTM F75 and F2068) femoral heads for wear testing. Two additional groups of acetabular liners ( $\text{Ø}28$  mm and  $\text{Ø}40$  mm) were fabricated from GUR 1050 UHMWPE, gamma irradiated at 78.5 kGy in inert gas, and subsequently annealed in nitrogen at 85–90 °C for 24 h. These XLPE liners were also terminally EO sterilized prior to coupling them with their respective  $\text{Si}_3\text{N}_4$  femoral heads. Prior to wear testing, all liners were subjected to accelerated ageing in accordance with ASTM F2003. After ageing, liners were placed in bovine serum (Sigma-Aldrich, St. Louis, MO, USA) at 37 °C to presoak. The serum was stabilized with 10.7 mmols of EDTA (Fisher Scientific, Pittsburgh, PA USA) and 33 mL of penicillin-streptomycin solution (Sigma-Aldrich) per 500 mL of serum, which was subsequently diluted with deionized water (Fisher Scientific) to 25% bovine serum per ISO 14242-1. Liners subjected to pre-soaking in bovine serum were weighed every three days until the weight change between the last two measurements exhibited less than 1%. At initiation and completion of wear testing, liners were measured for roundness using a scanning coordinate measuring machine (CMM, Global A2, Brown & Sharpe, Inc., North Kingston, RI, USA). Measurements were repeated three times for each component. Statistical differences in roundness were calculated using Student's *t*-tests with a significance threshold of  $p < 0.05$ . Mean surface roughness values ( $R_a$ ) for the femoral heads were measured before and after testing using a contact profilometer (Taylor Hobson Form Talysurf, Leicester, UK).

A 12-station hip simulator (Advanced Mechanical Technology, Inc., Watertown, MA, USA, or AMTI) was used to perform wear testing at 1 Hz for  $5 \times 10^6$  cycles using triaxial motion in an anatomical 30° cup angle position. A total of 18 femoral head and acetabular liner pairs were tested, twelve of which were subjected to both motion and load. The remaining pairs (1  $\text{Ø}28$  mm PE liner coupled with a CoCr femoral head, 3  $\text{Ø}28$  mm PE liners coupled with  $\text{Si}_3\text{N}_4$  femoral heads, and

2 Ø40 mm XLPE liners coupled with Si<sub>3</sub>N<sub>4</sub> femoral heads) were subjected to load without motion. These “load-soak components” were used to correct for fluid uptake into the PE and XLPE during testing. Fluid uptake from the Ø28 mm load soak pairs were averaged, and this average used to correct weight changes for all Ø28 mm PE liners, regardless of their coupled femoral head material. A standard walking gait cycle as specified in ISO 14242-1 was used. All stations were temperature controlled at 37 °C with circulating bovine serum, stabilized, and diluted as described previously. The serum was changed every half-million cycles, with interruptions for gravimetric wear measurements occurring at 0.5, 1, 1.5, 2, 3, 4, and 5 million cycles (Mc). Prior to weighing, liners were cleaned by brushing large debris off with a soft toothbrush, then sonicating them in a soap solution for 10 min, followed by drying. Each liner was weighed three times using a precision balance (XP205DR, Mettler-Toledo, Inc., Columbus, OH, USA) and the three weights were averaged. Photographs were obtained for each liner using stereo-optical microscopy (Zeiss AxioCam, ICc 1 digital camera and V8 microscope, Carl Zeiss, Thornwood, NY, USA). The weight loss of each liner was corrected for fluid absorption by subtracting the average weight gain of the load-soak components from the weight change of the motion components of the same size, material, and design. Gravimetric loss was converted to volumetric wear using a density of 0.938 g/cc for PE. Linear regression of the wear was correlated from 0.5 Mc to 5 Mc. Statistical differences between groups were calculated using Student’s *t*-tests, with a significance of  $p < 0.05$ . Wear particles were isolated from the collected serum by first diluting it with DI water to 50 vol %, adding proteinase K (Fisher Scientific), and stirring under heat (37 °C) for 45 min to digest proteins. This solution was further diluted to 10 vol % with DI water and filtered through an Isopore™ 0.2 µm membrane (Millipore, Billerica, MA, USA). The collected particles, consisting solely of PE, were gold-coated (108 Auto Sputter Coater, Cressington Scientific Instruments, Ltd., Watford, UK) and examined via SEM (FEI/Philips XL30 FEG ESEM, Hillsboro, OR, USA) at 20 kV. More than 140 particles per sample were analyzed for their equivalent circular diameter and inverse aspect ratio (i.e., width/length) to assess sphericity.

Upon completion of the wear test, four of the Ø28 mm XLPE liners were analyzed by Raman spectroscopy for changes in polyethylene crystallinity, including three subjected to both motion and load with the fourth liner being a load soak control. This spectroscopic assessment was made by means of a Raman microprobe spectrometer (T-64000, Horiba/Jobin-Yvon, Kyoto, Japan) in back-scattering geometry. The excitation source was a 488 nm Ar-ion laser (Stabilite 2017-Spectra Physics, Mountain View, CA, USA) yielding a power of approximately 35 mW on the UHMWPE liner surface. The confocal configuration of the probe corresponded to a 100× objective with the numerical aperture, focal length, and pinhole diameter fixed at NA = 0.9,  $f = 11$  mm, and  $\text{Ø} = 100$  µm, respectively. Spectra were typically collected during 10 s in non-polarized measurements. The recorded spectra were averaged over three successive measurements at each selected point. A spectral resolution better than  $0.15 \text{ cm}^{-1}$  was achieved by means of a 1800 grating L/mm. Spectral mapping was non-destructively performed in order to analyze the microstructure of the polymer down to 100 µm inside of the acetabular liner. Statistically meaningful characterizations of the three wear-tested liners were obtained by averaging the data retrieved from four different locations in both the worn area (hereafter referred to also as wear zone) and the non-contact area (hereafter referred to also as non-wear zone). The inclination angle of the liner within the simulator (i.e., 30°) was taken into account when selecting the non-wear zone areas for analysis. For each selected location, a map  $50 \times 50 \text{ µm}^2$  in dimension was collected at six different depths (0, 5, 10, 25, 50, and 100 µm) with an in-plane sampling of 2.0 µm step (for a total of 676 spectra per each map), as shown in Figure 1. Two locations on the dome and two locations on the assumed non-contact area were also selected for analyses on the load soak liner (hereafter referred to as the “pristine liner”). The relationship between the observed Raman bands and the vibrational modes of the polyethylene molecular structure has been amply documented in the literature [38–43]. Spectral deconvolutions were performed by means of an automatic fitting algorithm enclosed in a commercially available computational package (Labspec 5, Horiba/Jobin-Yvon, Kyoto, Japan) using mixed Gaussian-Lorentzian curves.

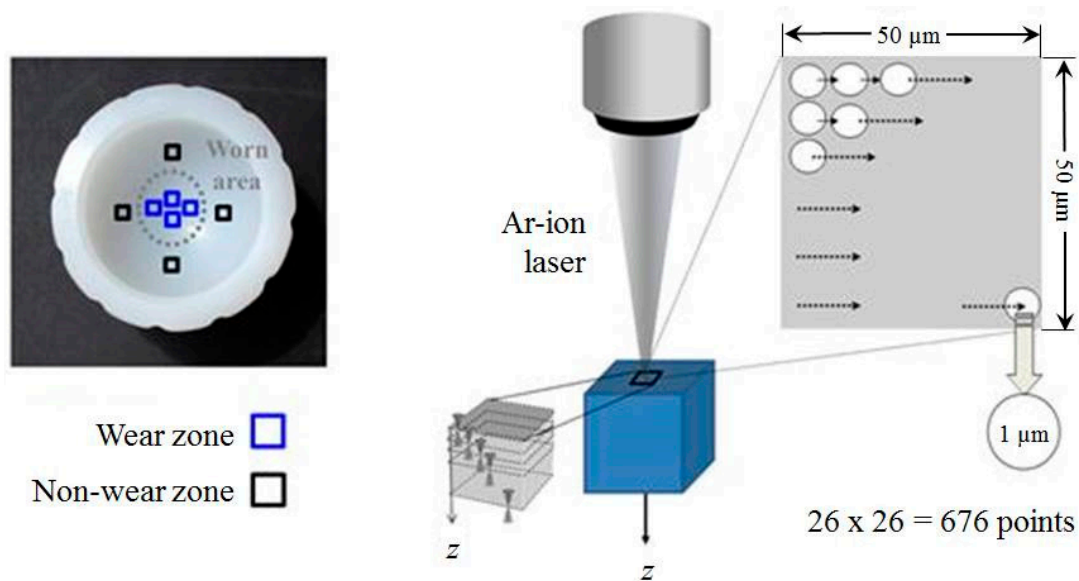


**Figure 1.** Schematics showing the location of the liners selected for spectroscopic analysis and the adopted mapping protocol.

The fractions of orthorhombic crystalline ( $\alpha_c$ ) and amorphous ( $\alpha_a$ ) phases were calculated from the Raman spectrum of polyethylene, according to the following equations [43]:

$$\alpha_c = \frac{I_{1414}}{0.46 (I_{1293} + I_{1305})} \quad (1)$$

$$\alpha_a = \frac{I_{1080}}{0.79 (I_{1293} + I_{1305})} \quad (2)$$

where  $I$  is the integral intensity of each individual Raman band identified by the subscript (i.e., after spectral deconvolution). Note also that the sum ( $\alpha_a + \alpha_c$ ) might locally be  $<1$ , because of the possible presence of a minor fraction of matter in an anisotropic intermediate state (i.e., usually referred to as the “third phase”) [40,44]. Accordingly, the fraction of this intermediate phase,  $\alpha_t$ , can be expressed as follows:

$$\alpha_t = 1 - (\alpha_c + \alpha_a) \quad (3)$$

Equations (1)–(3) constitute the basis of the Raman spectroscopic method for characterizing the crystalline structures of the UHMWPE. Two-dimensional Raman maps were collected at different focal depths of each liner. Two tailed Student  $t$ -tests (95% confidence,  $p < 0.05$ ) were used to compare population means at different depths of the pristine and wear-tested liners in their respective wear and non-wear zones.

## 2.2. SWM Ceramic-on-Polyethylene Hip Simulator Study

Wear testing in this study was conducted in accordance with ISO 14242-3 with the following specific differences. Only isostatically molded Ø28 mm GUR 1050 PE liners which were gamma sterilized at 25–40 kGy in an inert gas were used and paired with Si<sub>3</sub>N<sub>4</sub> (MC<sup>2</sup>®, Amedica, Salt Lake City, UT, USA) [37] and CoCr (ASTM F75 and F2068) femoral heads. Prior to wear testing, all PE liners (including controls) were soaked in DI water at room temperature until there was no observable weight change. Liner wear was measured gravimetrically (Sartorius Precision Balance, Bohemia, NY, USA) per ASTM 1714 and adjusted using an average of six load-soak controls. Gravimetric loss was converted to volumetric wear as indicated previously, and regression analyses were used to compare groups at significance of  $p < 0.05$  via Student’s  $t$ -tests. All PE liners were placed in an inverted position

at a 30° cup angle in a 9-station biaxial rocking motion hip simulator (Shore-Western, Monrovia, CA, USA, or SWM) for 5.0 Mc of normal gait based on a standard Paul curve (i.e., 2.2 kN max; 0.2 kN min, 1.0 Hz). The lubricant was alpha-calf serum (HyClone, Logan, UT, USA) diluted with DI water to obtain a protein concentration of 20 mg/mL and a pH of 8.0. EDTA was added (20 mL per L) to reduce calcium film in accordance with previous studies [45]. A bactericide was not added to the lubricant; but it was changed every 0.5 Mc. Testing was interrupted at 1.0, 3.0, and 5.0 Mc to assess wear. All components were cleaned and weighed using ASTM F1714 protocol. Regression analysis was used to calculate average wear rates, and Student's *t*-tests were used to compare groups and significance. Surface roughness ( $R_a$ ) was acquired for the  $\text{Si}_3\text{N}_4$  and CoCr femoral heads and liners using a non-contact surface analyzer (New View 5000, Zygo, Middlefield, CT, USA) in three random polar positions. Initial surface roughness of the CoCr heads was not measured prior to testing, but values were acquired at each stoppage for wear assessment. Optical (BX41, Olympus America, Center Valley, PA, USA) and scanning electron microscopy (SEM, Quanta, FEI, Hillsboro, OR, USA) were selectively conducted on the wear-tested components. All samples were sputter-coated (108 auto, Cressington, Watford, UK) with a thin (~20 to 30 Å) layer of gold. Samples were imaged using an accelerating voltage of 10 kV at working distances of 7–10 mm and spot sizes of 4–5 mm.

### 2.3. SWM Ceramic-on Ceramic Hip Simulator Study

In this study, six Ø28 mm and three Ø40 mm matched  $\text{Si}_3\text{N}_4$  head and liner pairs ( $\text{MC}^2$ ®, Amedica Corporation, Salt Lake City, UT, USA) [37] along with three similar Ø28 mm  $\text{Al}_2\text{O}_3$  (BIOLOX® forte, CeramTec, Plochingen, Germany) [46] pairs were tested in a 12-station SWM hip simulator. All bearing pairs were run in an inverted mode with a 30° cup angle. Lubricant preparation was as indicated in Section 2.2, with change-outs occurring at every 0.5 Mc. Other parameters of this biaxial wear test were representative of ISO 14242-3. Gravimetric wear results obtained at 0.25, 0.5, 1, 1.5, 2, and 3 Mc were converted to volumetric wear using density values of 3.27 g/cc and 3.98 g/cc for  $\text{Si}_3\text{N}_4$  and  $\text{Al}_2\text{O}_3$ , respectively. Surface roughness, scratches, and protein deposition profiles were evaluated using the aforementioned non-contact surface analyzer. The standard ISO 14242-3 testing sequence was terminated at 3.0 Mc due to near zero wear and substantial protein build-up on the articulation components. In lieu of its completion, the test was altered to include two experimental factors: (1) A 35 s dwell was engineered into the test protocol at maximum load (cf. Figure 2); and, (2) Several experimental cleaning techniques were employed in an attempt to remove adsorbed proteins. The static dwell was selected because it appeared to be more clinically relevant than the 24/7 continuous Paul orbital duty cycle, given that patients function quite differently, with intermittent, multidirectional, and varied motion. It was envisaged that a dwell at constant load would likely expel serum lubricant from the contact zone between head and liner pairs requiring subsequent acceleration to overcome unlubricated static friction, with the combined effect of adverse wear for these hard-on-hard bearings. The experimental cleaning protocols were employed because of tenacious adherence of proteins to all the components. After removal of the implants from the simulator, they were imaged for deposits, and then soaked in DI water for 3 h to hydrate the proteins. They were subsequently placed in concentrated muriatic acid (i.e., HCl, at ~20%) and sonicated for 30 min. After removal from the acid bath they were rinsed with DI water, placed in an ethanol bath, and sonicated for an additional 15 min. Implants were then weighed and imaged for protein deposition and wear. After 3 Mc other cleaning methods were also tested, including the use of a commercial solvent (Microclean Multicare™ Microcare Corp., New Britain, CT, USA), multi-enzyme detergents (Enzyte™, Decon Labs, Inc., Bryn Mawr, PA, USA), and standard alkaline detergents. Wear testing was then resumed for an additional 2 Mc using the revised loading profile and cleaning methods. Wear particles were neither obtained nor analyzed from this CoC study.

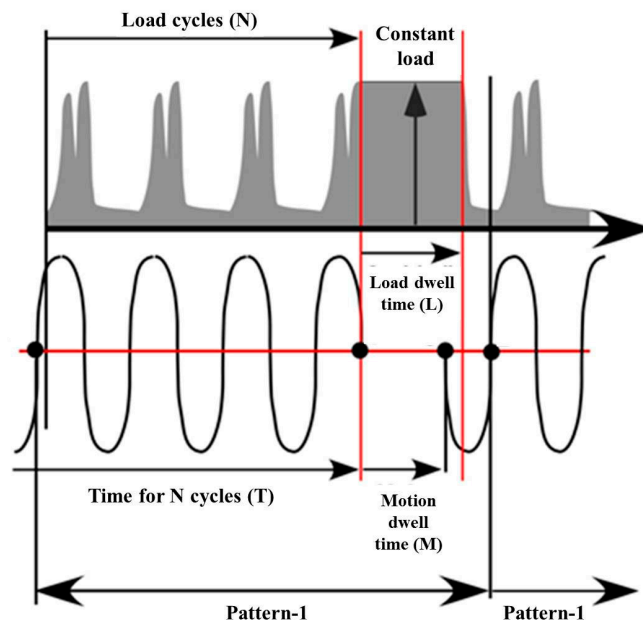


Figure 2. Modification of load and cycle profile for ceramic-on-ceramic SWM wear study.

### 3. Results and Discussion

#### 3.1. AMTI Ceramic-on-Polyethylene Hip Simulator Study

Given in Table 1 are wear results for hip simulator testing of Si<sub>3</sub>N<sub>4</sub> femoral heads against PE and XLPE liners, with comparisons to other biomaterials presented in Figure 3 [31,36,45,47–99]. For the AMTI study, volumetric wear rates for Ø28 mm PE acetabular liners articulating against CoCr and Si<sub>3</sub>N<sub>4</sub> femoral heads were 53.1 ± 4.8 mm<sup>3</sup>/Mc and 66.0 ± 5.8 mm<sup>3</sup>/Mc, respectively. This difference was statistically significant (*p* = 0.02), but, as will be discussed later, the lower wear rate for the CoCr femoral heads was likely due to greater protein adsorption onto the CoCr-PE wear couple as compared to the Si<sub>3</sub>N<sub>4</sub>-PE couple. Volumetric wear rates for the Ø28 mm and Ø40 mm XLPE liners articulating against Si<sub>3</sub>N<sub>4</sub> were 5.0 ± 1.3 mm<sup>3</sup>/Mc and 9.1 ± 1.6 mm<sup>3</sup>/Mc, respectively. There were no comparative controls for the XLPE liners used in the AMTI study.

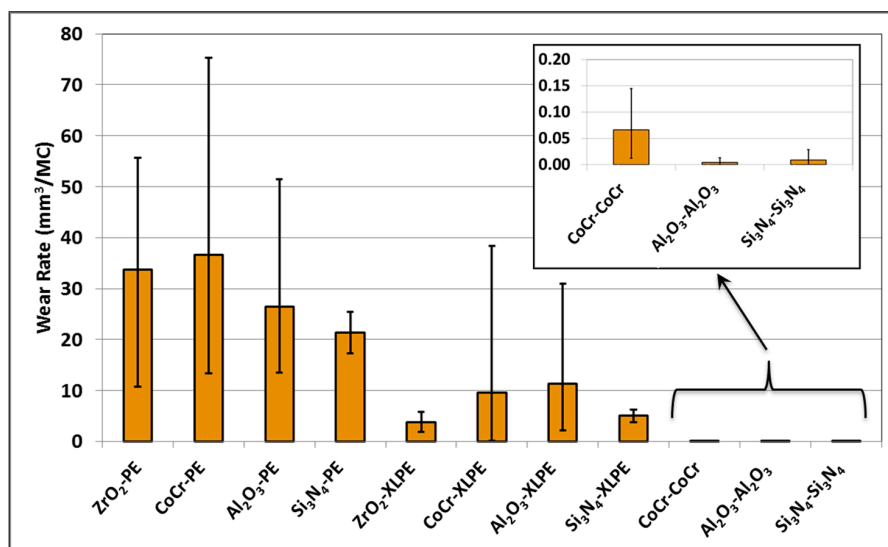
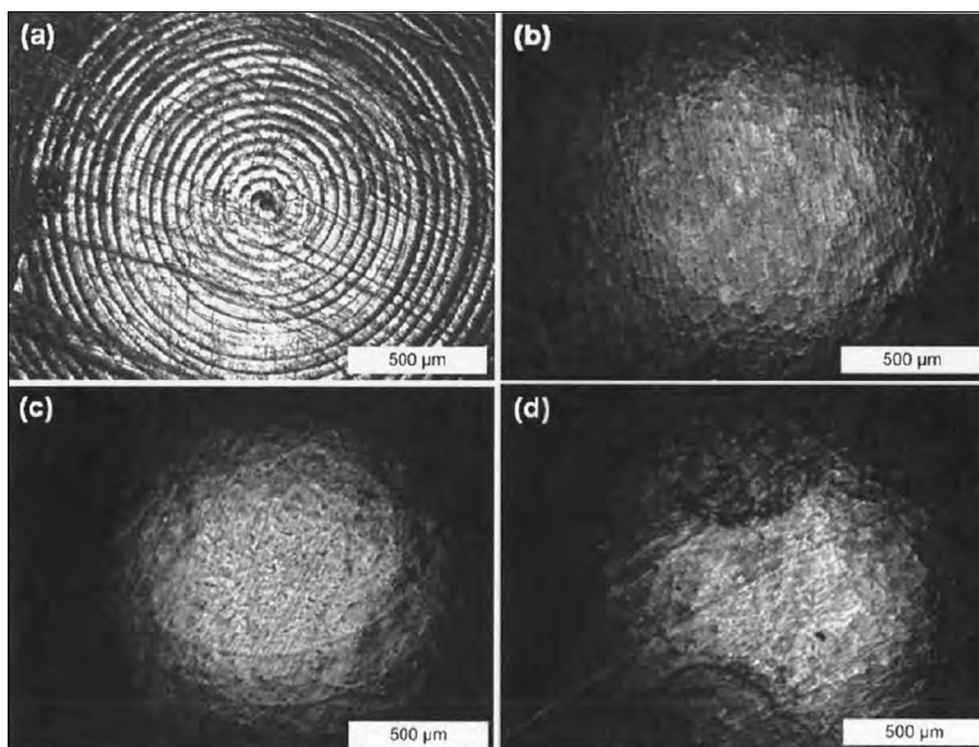


Figure 3. In vitro range of reported wear rates for various THA bearing materials [31,36,45,47–99].

**Table 1.** Polyethylene wear rates from AMTI and SWM simulators at 5 Mc.

Femoral Head Material	Testing Machine	Bearing Size	UHMWPE & Sterilization Method	Wear Rate (mm <sup>3</sup> /Mc)	Range (mm <sup>3</sup> /Mc)
Si <sub>3</sub> N <sub>4</sub>	AMTI	28	PE, ETO	66.0 ± 5.8	60.3–71.9
CoCr	AMTI	28	PE, ETO	53.1 ± 4.8	47.5–56
Si <sub>3</sub> N <sub>4</sub>	AMTI	28	XLPE, 78.5 KGy, ETO	5.0 ± 1.3	3.5–6.0
Si <sub>3</sub> N <sub>4</sub>	AMTI	40	XLPE, 78.5 KGy, ETO	9.1 ± 1.6	8.1–10.9
CoCr	SWM	28	PE, 25–40 KGy	17.6 ± 0.7	16.7–18.1
Si <sub>3</sub> N <sub>4</sub>	SWM	28	PE, 25–40 KGy	21.3 ± 4.1	16.7–24.3

As expected, the wear rate for the XLPE liners was significantly lower ( $p = 0.001$ ) than the PE liners, regardless of size; and the wear rate for the Ø40 mm XLPE liners was greater ( $p = 0.01$ ) than that of the Ø28 mm XLPE liners. Bulk lubricant temperatures monitored throughout the test showed no significant differences between any of the cells, typically ranging between  $37.7 \pm 0.5$  °C and  $37.9 \pm 0.2$  °C. There were no changes in the roundness of any of the liners after 5 Mc as measured by CMM. Photographs of PE components (cf. Figure 4) showed an immediate disappearance of most of the machining marks after 0.5 Mc. Between 3.0 and 5.0 Mc, the surfaces showed marked adhesive wear, which is typical of conventional PE. Photographs of the XLPE liners (cf. Figure 5) also showed early disappearance of machining marks. However, they were still distinguishable after 0.5 Mc, but essentially removed at  $\geq 2.0$  Mc. The particle analysis revealed no significant differences in size between any of the groups (cf. Figure 6). Particles from XLPE liners were, in general, slightly rounder than particles from PE liners, exhibiting a larger average inverse aspect ratio, although this difference was not statistically significant. No CoCr or Si<sub>3</sub>N<sub>4</sub> wear debris was observed in these AMTI tests. Mean surface roughness values ( $R_a$ ) for CoCr and Si<sub>3</sub>N<sub>4</sub> heads were not significantly different, ranging between  $11.9 \pm 1.6$  nm and  $14.2 \pm 3.2$  nm, respectively, after 5.0 Mc.



**Figure 4.** Photographs of PE liners from AMTI study at (a) 0 Mc; (b) 0.5 Mc; (c) 2 Mc; and (d) 5 Mc. All photos were taken at the dome of the component.

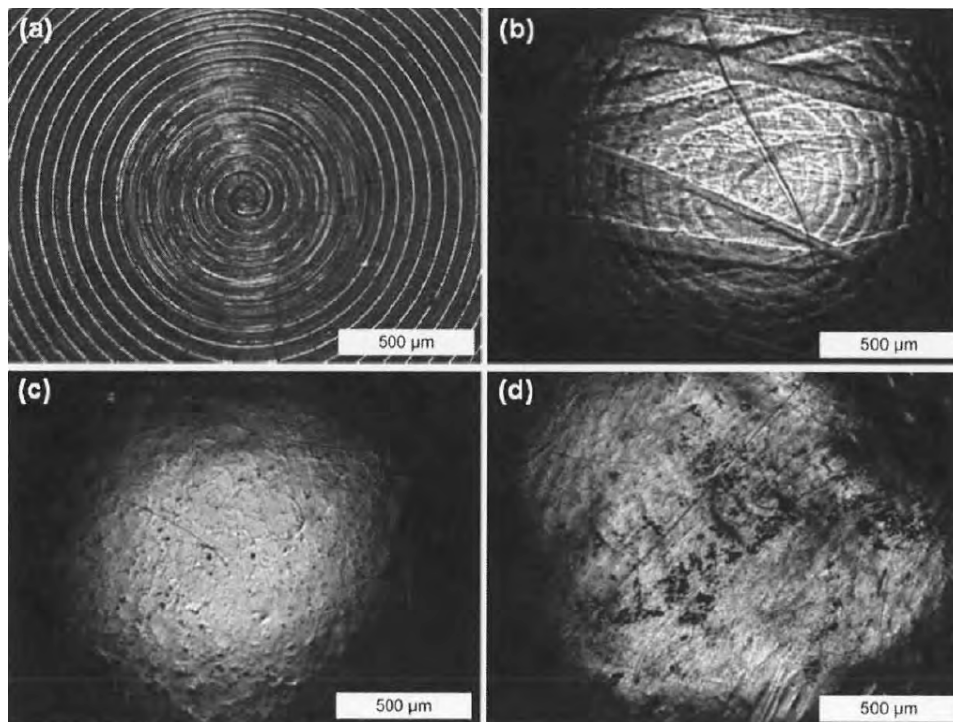


**Figure 5.** Photographs of XLPE liners from AMTI at (a) 0 Mc; (b) 0.5 Mc; (c) 2 Mc; and (d) 5 Mc. All photos were taken at the dome of the component.

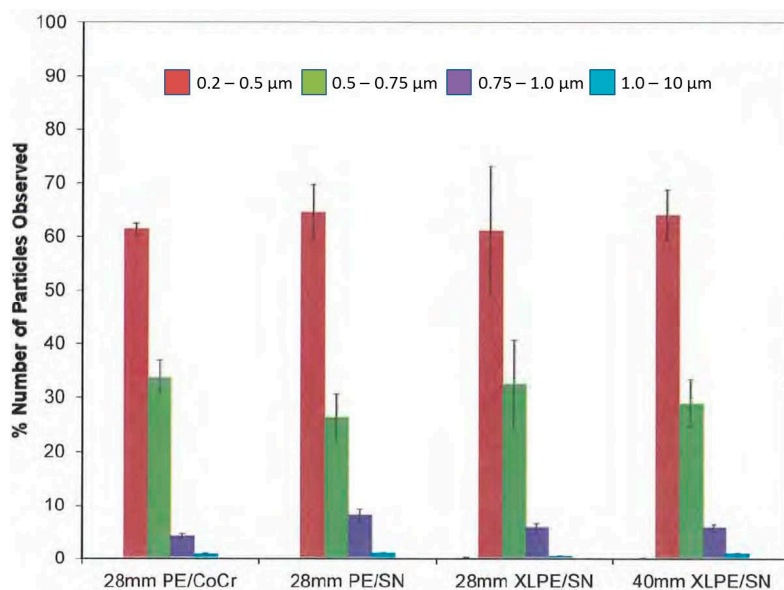


**Figure 6.** Wear particle distribution of the four different groups from the AMTI Study. The graph represents size distribution only, and is not indicative of total or cumulative particle counts.

The Raman spectroscopic results of the AMTI liners are shown in Figure 7. Average phase fraction profiles (i.e., crystalline, amorphous, and third phase) are compared for wear, non-wear, and pristine zones of the liners. For all analyzed samples, the crystalline phase increased within the first few microns of the subsurface, and reached a plateau at a depth of around 50 μm. While this trend is typical for other commercial UHMWPE liners, there was a significant difference between wear, non-wear, and the pristine zones up to a depth of about 20 μm. Beyond 20 μm, the wear and non-wear zones showed similar crystalline phase contents, both of which were about 3% higher than the pristine

liner. Increased crystallinity was induced by formation of residual free radicals inside the amorphous phase. These reacted with oxygen, creating hydroperoxides, which evolved into ketones, carboxyl acids, and other carbonyl groups [100–102]. They are responsible for polyethylene chain breakage and subsequent recrystallization [103,104]. Recrystallization might have also been assisted by plastic deformation. Stretching and weakening of the crosslinks promotes reorganization of the polymeric structure and contributes to the formation of free radicals. In gamma-irradiated and artificially aged polyethylene, as is the case for these liners, more favorable conditions for oxidation are expected deeper within the liner as compared to the surface [105–108]. This might explain the negligible increase of crystallinity on the unworn surface. Within the first few microns of the subsurface, the pristine and non-wear zones showed similar amounts of amorphous and third phases, whereas there was a clear decrease of the third phase and increase of the amorphous phase for wear-zones. This suggests that both recrystallization and amorphization of the polymer occurred due to sliding against  $\text{Si}_3\text{N}_4$ . Amorphization appears to have increased at the expense of the third phase. Plastic deformation occurring in the superficial layer of the bearing may have induced rotation of the crystalline lamellae, which might have altered the molecular arrangement of the chains in the third phase, with a consequent increase in the amorphous phase. Overall, the wear-induced microstructural modifications of the polymer were small. The narrow increase in crystallinity within the subsurface of both wear and non-wear zones indicates that oxidative degradation is not severe, and that  $\text{Si}_3\text{N}_4$ 's natural affinity for oxygen may be beneficial in limiting degradation of XLPE liners [109]. In fact, recent *in vitro* accelerated hydrothermal ageing studies indicate that  $\text{Si}_3\text{N}_4$ 's ability to scavenge oxygen from the tribolayer may delay the onset of polyethylene embrittlement [110]. Clinically, this could ultimately lead to enhanced XLPE longevity. However, this observation must be confirmed by additional hip simulator testing and further analyses.

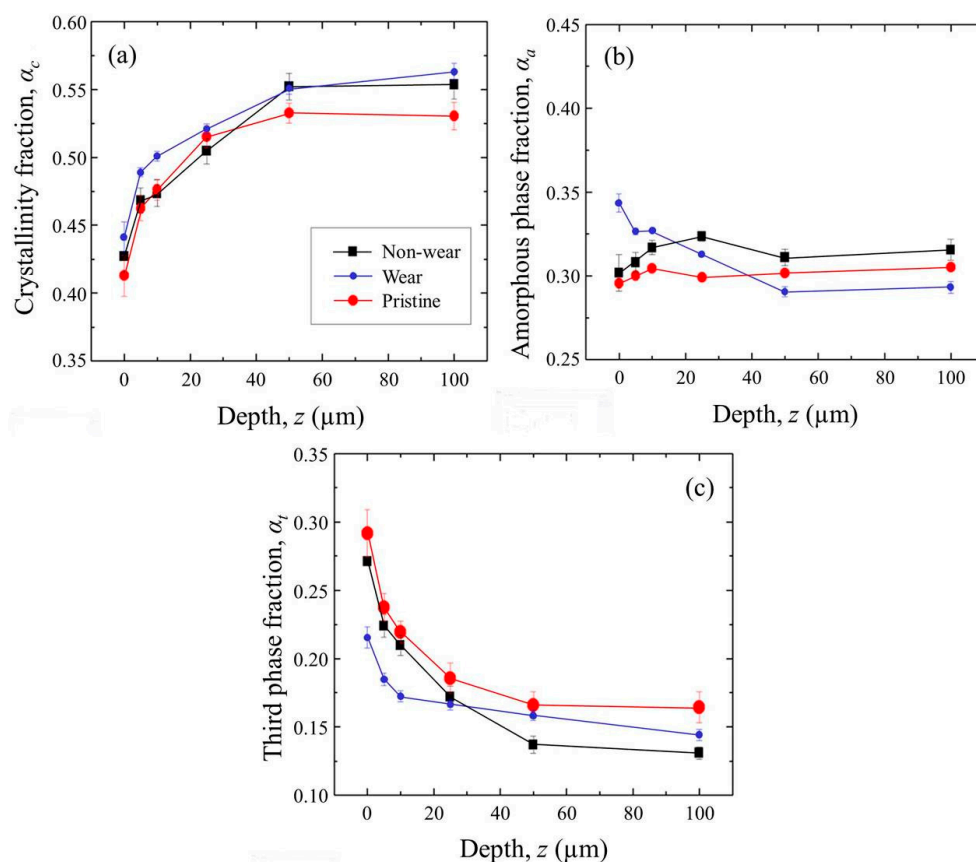


**Figure 7.** In-depth profiles of crystalline (a); amorphous (b); and third (c) phase fractions as obtained from the wear zone, non-wear zone, and the surface of the pristine liners from the AMTI wear study.

### 3.2. SWM Ceramic-on-Polyethylene Hip Simulator Study

Wear results for the SWM hip simulator testing of Si<sub>3</sub>N<sub>4</sub> femoral heads against PE are also given in Table 1, with comparisons to other biomaterials in Figure 3 [31,36,45,47–99]. In this study, volumetric wear rates for the PE liners were  $17.6 \pm 0.7 \text{ mm}^3/\text{Mc}$  and  $21.3 \pm 4.1 \text{ mm}^3/\text{Mc}$  for CoCr and Si<sub>3</sub>N<sub>4</sub> femoral heads, respectively. However, unlike the results from the AMTI study, this difference was not significant ( $p = 0.2$ ). Nevertheless, the observed lower wear rate for PE articulation against CoCr is consistent with observations from the AMTI study. In contrast to the AMTI study, there was a 4 °C higher average bulk lubricant temperature for cells containing CoCr versus Si<sub>3</sub>N<sub>4</sub> femoral heads in the SWM simulator. Also, in contrast to the AMTI study, surface finishes for both femoral heads in the SWM study increased throughout the test. This increase was significant ( $p = 0.01$ ) for CoCr femoral heads when compared to the Si<sub>3</sub>N<sub>4</sub> heads (cf. Table 2). For instance, at 1.0 Mc, the mean surface roughness ( $R_a$ ) of the Si<sub>3</sub>N<sub>4</sub> and CoCr femoral heads was 4.3 nm and 8.6 nm, respectively. At 5.0 Mc, the mean surface roughness of the Si<sub>3</sub>N<sub>4</sub> heads had increased to 15 nm, whereas the CoCr femoral heads had increased 7.5-fold to 112 nm. Despite the use of a common cleaning technique, optical and scanning electron microscopy revealed more organic particulate debris adhering to the CoCr femoral heads than the Si<sub>3</sub>N<sub>4</sub> components. For the acetabular liners, there was a 30% difference in mean surface finish at 1.0 Mc between the Si<sub>3</sub>N<sub>4</sub> and CoCr groups; but there was little difference thereafter. No particle collection or size distribution analyses were performed for the SWM study.

**Table 2.** Mean surface roughness ( $R_a$ ) and maximum observed roughness of femoral heads and acetabular liners from the SWM study (nm).

# of Cycles	Femoral Heads				Acetabular Liners			
	Si <sub>3</sub> N <sub>4</sub> Group		CoCr Group		Si <sub>3</sub> N <sub>4</sub> Group		CoCr Group	
	Mean	Max	Mean	Max	Mean	Max	Mean	Max
1 Mc	4.3	7	8.6	19	77	177	106	276
3 Mc	18	37	101	381	76	177	99	199
5 Mc	15	24	112	410	93	190	102	187

Testing differences between various laboratories using alternative hip simulators is an obvious source of variation in reported wear data, even with identical PE materials and protocols. Many machine variables remain controversial, such as simulator kinematics and their complexity, load application, utilization of a stationary head and moving liner or vice-versa, head on top or liner on top, multiple versus single station controls, lubricant composition, temperature, and circulation methods, among others [35]. Furthermore, a number of critical reviews have pointed-out the limitations of the accepted hip simulator testing standards (i.e., ISO 14242-1,3). They currently do not account for common clinically relevant conditions such as microseparation, malpositioning and edge loading, starved lubrication, and stop-motion, rest, and resume-motion sequences [111–113]. Each of these conditions has been shown to profoundly affect component wear and longevity.

The lower PE wear rates for test cells containing Ø28 mm CoCr femoral heads in both the AMTI and SWM studies are likely due to a combination of protein precipitation and preferential adhesion of UHMWPE debris. Protein adsorption onto bearing surfaces can be thermally or mechanically activated (i.e., frictional heating, pressure, or high shear) [114,115]. Their presence is often difficult to detect (<250 nm), but their effect in reducing wear has been extensively examined [45,62,116–125]. The temperature differential between CoCr and Si<sub>3</sub>N<sub>4</sub> cells within the SWM study suggests higher precipitation occurred in the CoCr cells. Even though no bulk differences in serum lubricant temperatures were observed in the AMTI study, it has been shown that the local interfacial surface temperature between the head and the liner can vary greatly depending upon the thermal conductivity of the head material. This effect was separately documented by Lu et al. [118] and Bowsher et al. [62]. In a hip simulator equipped with calibrated thermocouples, and with the aid of finite element analyses,

Lu et al. estimated transient interfacial temperatures between ZrO<sub>2</sub>, CoCr, and Al<sub>2</sub>O<sub>3</sub> femoral heads and PE liners of 99 °C, 60 °C, and 45 °C, respectively. These values inversely correlated with each head material's thermal conductivity [118]. Bowsher et al. studied the effect of femoral head thermal conductivity on PE wear rates for zirconia ZrO<sub>2</sub>, CoCr, Al<sub>2</sub>O<sub>3</sub>, and Si<sub>3</sub>N<sub>4</sub> and found logarithmic correlation with a coefficient of >0.99 [62]. Significant wear rate reductions were noted for the lower thermal conductivity materials. Thus, the CoCr heads, which ran demonstrably hotter in the SWM study, likely induced greater protein precipitation, resulting in reduced PE wear when compared to the Si<sub>3</sub>N<sub>4</sub> heads. Furthermore, although bulk serum temperatures in the AMTI study were consistent between CoCr and Si<sub>3</sub>N<sub>4</sub> cells, higher interfacial temperatures for cells containing CoCr heads also likely induced localized protein precipitation, which in turn reduced PE wear. Another possible reason for the lower UHMWPE wear rates using CoCr femoral heads could be due to adhesive as opposed to abrasive wear. Instead of wear debris being freely released into the lubricant by abrasion, it may have been adhesively retained on the femoral heads. Optical and SEM examination of the heads revealed rougher surfaces for the CoCr components (cf. Table 2) associated with a greater adherence of organic particulate debris. Similar to protein precipitation, adhesive wear is sensitive to interfacial temperature and friction [126]. Given the lower thermal conductivity of CoCr as compared to Si<sub>3</sub>N<sub>4</sub>, a large amount of polyethylene debris apparently adhered to the CoCr heads due to thermally activated adhesive wear. This effect was also apparent on the Si<sub>3</sub>N<sub>4</sub> heads, but to a lesser extent. As demonstrated by other investigators, the presence of serum proteins initially serves to reduce adhesive wear; but upon their precipitation, adhesion increases [118]. Furthermore, it has been demonstrated that CoCr has a propensity for greater polyethylene adhesive wear than nitride-based materials [127].

Figure 3 presents comparative PE and XLPE wear data for gamma irradiated UHMWPE liners articulating against CoCr, ZrO<sub>2</sub>, Al<sub>2</sub>O<sub>3</sub>, and Si<sub>3</sub>N<sub>4</sub> femoral heads. These data were extracted from a survey of peer-reviewed publications, comprising approximately 60 hip simulator studies dating from the mid-1990s to the present [31,36,45,47–99]. Results from the AMTI and SWM studies are included in the figure; but data from the ETO-only sterilized PE of the AMTI study were omitted due to a paucity of comparative literature and its current clinical irrelevance. Nowadays, most PEs are gamma irradiated to form XLPE, and if not, they are gamma sterilized. The highest polyethylene wear rates reported in the literature are typically for non-irradiated PEs. Yet, even low amounts of radiation initiate cross-linking, which in turn results in significant wear reductions. This effect was aptly demonstrated by Wang et al. [128]. For non-irradiated polyethylene, they reported a PE wear rate of ~140 mm<sup>3</sup>/Mc against 32 mm CoCr. An irradiation dosage of as little as 25 kGy reduced the wear rate by over 60% to 50 mm<sup>3</sup>/Mc, which is typical of the values observed in Figure 3. Further irradiation was even more effective, reducing the wear rate to 1/20th that of a non-irradiated polymer. Therefore, gamma sterilization of the SWM Ø28 mm PE liners is likely a major factor in their observed lower wear rates in comparison to the AMTI PE liners. Nevertheless, there is a broad range of reported PE wear rates for various bearing couples; and it is evident that even mildly irradiated PE can eclipse the ETO-only sterilized PE wear performance from the AMTI study. Wear rates decrease asymptotically for the highly cross-linked XLPE (>75 kGy) as demonstrated in the AMTI study (cf. Table 1); and compiled data from Figure 3 indicate that Si<sub>3</sub>N<sub>4</sub>-on-XLPE couples have comparable XLPE wear to CoCr and Al<sub>2</sub>O<sub>3</sub> containing bearings [31,36,45,47–99]. Therefore, data from both the AMTI and SWM studies for PE and XLPE liners can be considered consistent with the range of reported wear rates from published literature. In summary, both the AMTI and SWM studies showed greater UHMWPE wear when articulating against Si<sub>3</sub>N<sub>4</sub> femoral heads. However, the wear differential for the SWM study was not statistically significant. Furthermore, considering the observed confounding effects of preferential protein adsorption and polyethylene debris adhesion to the CoCr femoral heads, it was concluded that the UHMWPE wear using Si<sub>3</sub>N<sub>4</sub> was likely at least equivalent to CoCr. Overall, these results indicate that Si<sub>3</sub>N<sub>4</sub> femoral heads can be effectively used in CoP total joint arthroplasty devices, and suggest that oxidative protection of the polyethylene may be an added benefit.

### 3.3. SWM Ceramic-on-Ceramic Hip Simulator Study

Head, liner, and combined volumetric wear rates for the SWM CoC hip simulator study at 3.0 Mc are provided in Table 3. For Ø28 mm couples, there were no significant differences in wear rates between Si<sub>3</sub>N<sub>4</sub> and Al<sub>2</sub>O<sub>3</sub> bearings, with both essentially showing near zero wear. In fact, within experimental error, the Ø28 mm femoral heads had a slight weight gain whereas their corresponding liners indicated an opposite trend. As expected, there was more wear with Ø40 mm Si<sub>3</sub>N<sub>4</sub> couples than either the Ø28 mm Si<sub>3</sub>N<sub>4</sub> or Al<sub>2</sub>O<sub>3</sub> bearings, leading to significant differences in head ( $p = 0.02$ ) and combined ( $p = 0.05$ ) wear rates, but, interestingly, no differences in liner wear rates. The Ø40 mm Si<sub>3</sub>N<sub>4</sub> heads and liners showed continual, but minimal material loss throughout the 3.0 Mc test. There were no Ø40 mm Al<sub>2</sub>O<sub>3</sub> controls included in this simulator study. The wear performance of Si<sub>3</sub>N<sub>4</sub> and Al<sub>2</sub>O<sub>3</sub> bearings in this study are comparable to compiled data for other hard-on-hard bearings (cf. Figure 3), and both are superior to CoCr-on-CoCr bearings.

**Table 3.** Ceramic-on-ceramic wear rates from SWM hip simulator at 3 Mc. (Negative values indicate volumetric material loss).

Material	Bearing Size	Wear Rate (mm <sup>3</sup> /Mc)		
		Head	Liner	Combined
Silicon Nitride	28 mm	0.007 ± 0.009	−0.014 ± 0.017	−0.007 ± 0.017
Alumina	28 mm	0.004 ± 0.013	−0.020 ± 0.012	−0.017 ± 0.012
Silicon Nitride	40 mm	−0.023 ± 0.003	−0.029 ± 0.022	−0.052 ± 0.014

Protein precipitation was suspected as the source of the observed weight variability of these bearing couples. Consequently, the standard ISO-prescribed study was interrupted at 3.0 Mc. The components were examined for protein deposition at that point, followed by experimenting with several cleaning methods. Shown in Figure 8a is the wear pattern observed on one of the Si<sub>3</sub>N<sub>4</sub> femoral heads at 3.0 Mc. This head exhibited a slight change in color over its entire surface (from a dark gray to lighter gray), but its appearance was more significant in the main wear zone (MWZ), and a rainbow of colors was seen in the transition zone (TZ). The results of non-contact white light interferometry for this head are shown in Figure 8b–d. Proteins are evident, appearing as adherent columnar structures of uniform thickness (~250 nm). Scratch patterns of approximately 200 µm in width were observed, which abrasively removed proteins down to the original ceramic surface. As described in the methods section, several experimental cleaning protocols were employed to remove the proteins. After each attempt, wear testing resumed using an interrupted loading profile (i.e., *stop-dwell-start*) as described previously, with the test eventually terminating at 5.0 Mc. Measurements taken during this non-standard segment showed heightened wear and variability. This is highlighted in Figure 9 for two each of Ø28 mm Si<sub>3</sub>N<sub>4</sub> and Al<sub>2</sub>O<sub>3</sub> femoral heads. Part of the observed variability was presumably due to protein precipitation and adhesion. Yet, even though there was greater variability, the wear for the Si<sub>3</sub>N<sub>4</sub> heads was statistically indistinguishable from the Al<sub>2</sub>O<sub>3</sub> controls. Conversely, presented in Figure 10 is combined average wear for all bearing materials and sizes. Note again from this figure that wear for Si<sub>3</sub>N<sub>4</sub> and Al<sub>2</sub>O<sub>3</sub> bearings up to three Mc was equivalent and essentially equal to zero. However, introduction of the *stop-dwell-start* loading cycle and alternative cleaning methods had a significant effect on the wear rate for Si<sub>3</sub>N<sub>4</sub> bearings, increasing the average for both Ø28 mm and Ø40 mm bearing pairs to 7.99 mm<sup>3</sup>/Mc and 2.93 mm<sup>3</sup>/Mc, respectively, while the Al<sub>2</sub>O<sub>3</sub> controls remained near zero wear. In particular, an abrupt loss of material was noted for two of six Si<sub>3</sub>N<sub>4</sub> bearings between 3.0 Mc and 5.0 Mc, (one each of Ø28 mm and Ø40 mm), whereas the remaining four Si<sub>3</sub>N<sub>4</sub> couples had essentially zero wear, comparable to the Al<sub>2</sub>O<sub>3</sub> couples. Reasons for this variability are presently unknown. It was initially postulated that perhaps it was due to lack of diametral conformity between the matched heads and liners, or related to differences in finish between convex and concave surfaces. However, post-test inspection provided no correlation, with clearances

ranging from 69  $\mu\text{m}$  to 156  $\mu\text{m}$ , and RMS  $R_a$  values of between 8 nm and 35 nm. Clearly, the contrasting use of the non-standard cycle, which included the hold sequence at maximum load, played a significant role in lubrication breakdown and increased friction. The *stop-dwell* segment likely expressed lubricant out of the contact area between the head and liner leading to a breakdown of fluid film and resumption of boundary layer lubrication. Contacting asperities between surfaces then dramatically increased static friction, leading to their microfracture upon re-start of the bearing. Indeed, scuffing, microcracks, and microfracture were observed on the high-wear  $\text{Si}_3\text{N}_4$  bearings. This wear pattern is consistent with the findings of other investigators who reported that heterogeneous acicular ceramic microstructures exhibit this type of wear behavior [129–131]. Thermally activated dissolution of the bearing surface (or wear debris) and reformation of the tribochemical film ensued which lowered friction, until the bearing once again came to its next *stop* in the cycle, resulting in a repetition of *stick-slip* behavior.

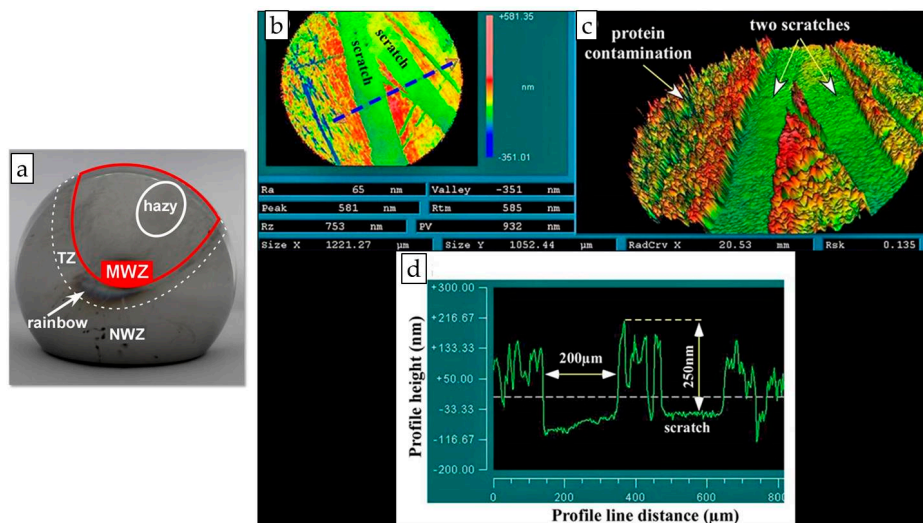


**Figure 8.** (a) Surface appearance of a  $\text{Si}_3\text{N}_4$  femoral head after 3 Mc; and non-contact white light interferometry and profilometry views of  $\text{Si}_3\text{N}_4$  femoral head demonstrating tenacious protein adhesion at 3 Mc; (b) mono-microscopic view; (c) stereo-microscopic view; and (d) scratch profiles.

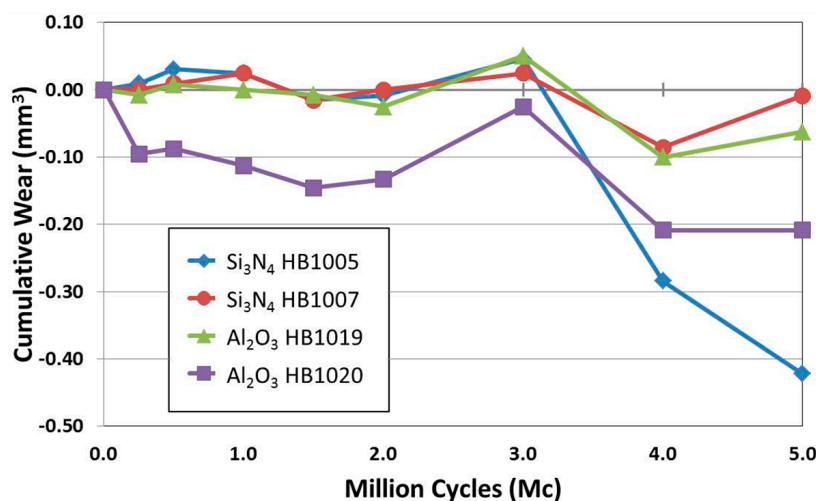


**Figure 9.** Wear of  $\text{Si}_3\text{N}_4$  and  $\text{Al}_2\text{O}_3$  femoral heads in ceramic-on-ceramic bearings.

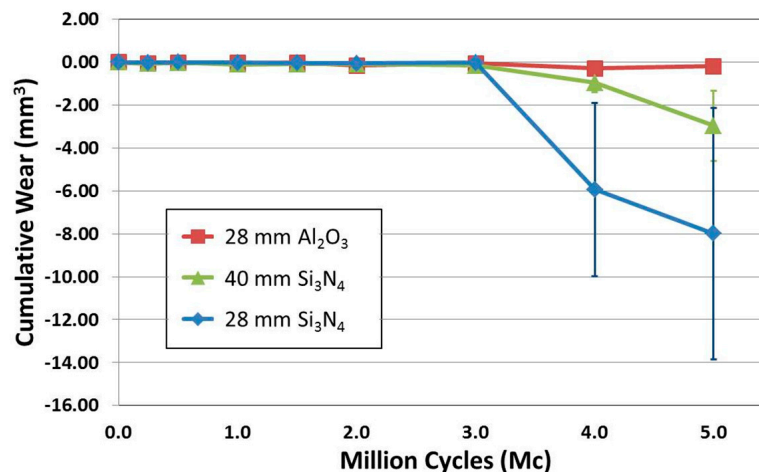
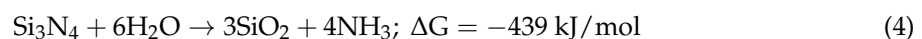


Figure 10. Cumulative wear results for ceramic-on-ceramic 5 Mc SWM study.

The collected data from the SWM CoC wear test provide three instructive points: (1) Frictional heating leads to serum degradation and protein precipitation on all bearing couples, which adversely affects observed weight or volumetric changes [62,111,132]. Consequently, hip simulator wear rates need to be tempered with the knowledge that bearing materials of dissimilar thermal conductivities may result in markedly different wear behavior; (2) While the standard Paul cycle is used for test expediency, continuous motion simulation does not adequately represent actual human gait [98,111,113,133]. Alternatively, a *stop-dwell-start* protocol is more clinically relevant, and may more effectively discriminate between bearing materials; and, (3) Interruption of the continuous Paul cycle leads to lubrication breakdown for Si<sub>3</sub>N<sub>4</sub> bearings, resulting in increased friction and wear.

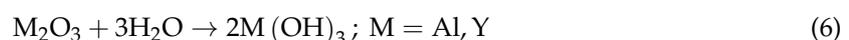
As discussed in the introduction, a significant number of studies have examined the friction and wear behavior of self-mated Si<sub>3</sub>N<sub>4</sub> in aqueous environments. In general, all prior research supports the observation that Si<sub>3</sub>N<sub>4</sub> wears via a hygroscopic tribochemical reaction. Surface transitional oxynitrides (–Si<sub>2</sub>NH, –SiNH<sub>2</sub>, –Si<sub>2</sub>ON<sub>2</sub>) [134] react with water to generate silicon dioxide (i.e. silica, or SiO<sub>2</sub>) and ammonia (NH<sub>3</sub>) in accordance with the following equation [135]:



However, instead of pure silica, it is now recognized that several intermediate hydrated meta- and orthosilicates form within the tribochemical film, the most prominent being silicic acid (Si(OH)<sub>4</sub>) in accordance with the following reaction [26]:



In its hydrated form, particularly in the presence of amines, alkali, or alkali-earth ions, silicic acid develops a viscous gel [136,137]. This gelatinous structure forms a coherent hydrodynamic film in the wear track, which serves as the primary lubrication source between bearing surfaces. Its presence dramatically reduces the bearing's dynamic friction coefficient. Even a more complicated picture ensues when accounting for the oxide sintering aids incorporated into Si<sub>3</sub>N<sub>4</sub> grain boundaries, or substituted into the silicon nitride lattice itself [138]. The probable tribochemical reaction for Si<sub>3</sub>N<sub>4</sub> containing Al<sub>2</sub>O<sub>3</sub> and Y<sub>2</sub>O<sub>3</sub> dopants is given in the following equation:



Equation (6) indicates that aluminum hydroxide is tribochemically formed during wear; and actually, this has been verified for Al<sub>2</sub>O<sub>3</sub> ceramics [139]. For yttria, a similar reaction is possible; but in accordance with Fisher et al., yttria likely forms insoluble fractured roll debris in the wear track [140]. Note that copious amounts of water are consumed during these tribochemical reactions

(i.e., Equations (4)–(6)). From an estimate of contact area and fluid film thickness (i.e.,  $\text{Ø}4$  to  $\text{Ø}6 \text{ mm}^2 \times 40$  to  $90 \text{ nm}$ , respectively) [141,142], part of the *stick-slip* behavior could be due to lubrication starvation, wherein insufficient local moisture is available to facilitate continued formation of the tribochemical film, resulting in an abrupt transition from hydrodynamic to boundary lubrication [143,144]. Observations from the SWM CoC hip simulator are in line with previously cited literature on the wear behavior of self-mated  $\text{Si}_3\text{N}_4$ . It is characterized by the following salient features:

- (1) High friction is initially observed during a transient run-in period; but this dramatically declines with increasing sliding distance due to formation of a coherent tribochemical lubricating film.
- (2) Reduced friction is maintained by continuous motion at lower loads and higher speeds. These conditions aid in retention of the tribochemical film within the wear track. However, slight perturbations of the wear couple (i.e., displacement of the bearing out of the normal wear track) result in an immediate increase in friction, returning the bearing to its transient run-in period. Reformation of the tribochemical film is necessary to reduce friction to prior low levels.
- (3) Conversely, high or oscillating friction, and *stick-slip* behavior are observed for high-loads (above a critical value), slow speeds, and *start-stop* cycling, as the bearing transitions from hydrodynamic to boundary film lubrication and back again; and,
- (4) The reaction products that form the tribochemical film are soluble and potentially resorbable.

Furthermore, this study suggests that current hip simulation standards inadequately represent the varied kinematics of the human gait. Common daily activities of standing, bending, walking, or running, coupled with rest periods of sitting or reclining, subject bearing couples to both a broad range of loads and repetitive *stop-dwell-start* cycles. The inclusion of a simplified stop-dwell-start sequence in this CoC study demonstrated a marked difference in bearing performance between  $\text{Al}_2\text{O}_3$ -on- $\text{Al}_2\text{O}_3$  and self-mated  $\text{Si}_3\text{N}_4$  bearings. This modest protocol change prevented the establishment of a coherent tribochemical fluid film, which appears to be essential for low-friction  $\text{Si}_3\text{N}_4$ -on- $\text{Si}_3\text{N}_4$  bearings. Instead, a hygroscopic reaction led to starved lubrication, which resulted in marked frictional fluctuations and higher wear. There are several possible solutions to this observed phenomenon. For example, aluminum ion implantation has been shown to increase  $\text{Si}_3\text{N}_4$ 's oxidation resistance. This treatment will likely improve  $\text{Si}_3\text{N}_4$ 's tribochemical performance as well [145–147]. Alternatively, coating  $\text{Si}_3\text{N}_4$  with a suitably engineered diamond-like carbon (DLC) is another relevant possibility. Enhanced bearing longevity can be expected provided an adherent defect free coating is achieved; and the elastic moduli of the substrate and coating are reasonably matched [148]. From another perspective, rigorous mechanical models (as well as market trends) suggest the use of dissimilar bearing materials in lieu of hard-on-hard devices (i.e., CoP vs. CoC) [149–151]. Due to differences in chemical affinities, elastic moduli, and hardness,  $\text{Si}_3\text{N}_4$ -on-XLPE bearings should not experience the same *slip-stick* behavior that was observed in the  $\text{Si}_3\text{N}_4$ -on- $\text{Si}_3\text{N}_4$  couples, although additional simulator testing needs to confirm this supposition. Additionally, in vivo studies demonstrate excellent wear performance and survivability (currently >10 years) for ceramic-on-XLPE in comparison to ceramic-on-ceramic articulation [152–155]. Further XLPE improvements (e.g., vitamin E stabilization or phospholipid grafting) along with lower costs will build on these advances, favoring continued use and future growth of CoP bearings [47,156–158].

#### 4. Summary and Conclusions

Since 2008  $\text{Si}_3\text{N}_4$  has proven to be an effective interbody fusion device in the cervical and thoracolumbar spine. Its success in this application has prompted an examination of its potential as a bearing material in total joint arthroplasty. Three separate wear studies were conducted for this purpose (i.e., two CoP and one CoC). For the CoP tests, average hip simulator wear for  $\text{Si}_3\text{N}_4$ -PE and -XLPE was found to be higher than CoCr controls. However, values were comparable to reported wear for similar polyethylenes using oxide ceramics. Protein precipitation on the lower thermal conductivity CoCr heads was found to be a confounding factor in interpretation of the wear data.

It is reasoned that the performance of Si<sub>3</sub>N<sub>4</sub> bearings against conventional PE or XLPE is at least equivalent to CoCr when accounting for this effect. No significant differences were observed in PE wear particles or PE surface morphology when using either CoCr or Si<sub>3</sub>N<sub>4</sub> femoral heads. Post-wear test Raman spectroscopic examination of an XLPE liner indicated that Si<sub>3</sub>N<sub>4</sub>'s natural affinity for oxygen might aid in preventing polyethylene degradation. For the CoC studies, Si<sub>3</sub>N<sub>4</sub>-on-Si<sub>3</sub>N<sub>4</sub> bearings had essentially zero wear up to 3.0 Mc in a continuous orbital motion duty cycle, and were statistically indistinguishable in performance to Al<sub>2</sub>O<sub>3</sub>-on-Al<sub>2</sub>O<sub>3</sub> controls. Protein adsorption onto the Si<sub>3</sub>N<sub>4</sub> couples was also noted in the CoC tests. However, in contrast to the self-mated Al<sub>2</sub>O<sub>3</sub> bearings, increased wear was observed for two Si<sub>3</sub>N<sub>4</sub> couples between 3.0 Mc and 5.0 Mc under a specially engineered load profile that incorporated a *stop-dwell-start* sequence. It is believed that this change resulted in the cyclic breakdown of fluid film, and resumption of boundary lubrication, with associated *slip-stick* behavior. This behavior is consistent with reported literature for self-mated Si<sub>3</sub>N<sub>4</sub> under water lubrication. A tribochemical reaction occurs upon initial abrasion of Si<sub>3</sub>N<sub>4</sub>'s oxynitride surface—the products being ammonia (NH<sub>3</sub>) and hydroxylated silicic acid (Si(OH)<sub>4</sub>·xH<sub>2</sub>O). Under low-loads, high speeds, and continuous motion, a coherent lubricating gelatinous film forms in the wear track; and this substantially reduces the bearing's friction and wear. However, high-loads, lower speeds and interrupted motion (or other perturbations) inhibit its formation, leading to increased or fluctuating friction and wear. Additional laboratory friction and hip simulator tests will be required to corroborate these observations, and ultimately clinical studies coupled with retrievals may be necessary to understand the potential of self-mated Si<sub>3</sub>N<sub>4</sub> couples. Nevertheless, the current results support the use of Si<sub>3</sub>N<sub>4</sub> against dissimilar surfaces (i.e., CoP); and further advancements in XLPE polymers are expected to accelerate the growth of CoP devices, including the potential use of Si<sub>3</sub>N<sub>4</sub> as a femoral head material.

**Acknowledgments:** John G. Bowsher (at Loma Linda University Medical Center), Brad R. Micheli, and Orhun K. Muratoglu (at Massachusetts General Hospital) are acknowledged for the simulator studies.

**Author Contributions:** R.L. conceived and designed the experiments; Wear testing was performed by the aforementioned laboratories; B.J.M., D.R., I.C.C., L.P., and G.P. analyzed the data; and, B.J.M., I.C.C., L.P., and G.P. wrote the manuscript.

**Conflicts of Interest:** B.J.M., A.L., and D.A.R. are employees of Amedica Corporation, a silicon nitride orthopaedic device manufacture. G.P. is a consultant to Amedica. None of the other authors has a financial or proprietary interest in the subject matter or materials discussed.

## References

1. Taylor, R.M.; Bernero, J.P.; Patel, A.A.; Brodke, D.S.; Khandkar, A.C. Silicon Nitride—A New Material for Spinal Implants. *J. Bone Jt. Surg. Br.* **2010**, *92*, 133.
2. Bal, B.S.; Rahaman, M. The Rationale for Silicon Nitride Bearings in Orthopaedic Applications. In *Advances in Ceramics—Electric and Magnetic Ceramics, Bioceramics, Ceramics and Environment*; INTECH Open Access Publisher: Rijeka, Croatia, 2011; pp. 421–432.
3. Bal, B.S.; Rahaman, M.N. Orthopedic Applications of Silicon Nitride Ceramics. *Acta Biomater.* **2012**, *8*, 2889–2898. [[CrossRef](#)] [[PubMed](#)]
4. Bal, B.S.; Khandkar, A.; Lakshminarayanan, R.; Clarke, I.; Hofmann, A.A.; Rahaman, M.N. Testing of Silicon Nitride Ceramic Bearings for Total Hip Arthroplasty. *J. Biomed. Mater. Res. Part B Appl. Biomater.* **2008**, *87*, 447–454. [[CrossRef](#)] [[PubMed](#)]
5. Bal, B.S.; Khandkar, A.; Lakshminarayanan, R.; Clarke, I.; Hofmann, A.A.; Rahaman, M.N. Fabrication and Testing of Silicon Nitride Bearings in Total Hip Arthroplasty. *J. Arthroplast.* **2009**, *24*, 110–116. [[CrossRef](#)] [[PubMed](#)]
6. Neumann, A.; Reske, T.; Held, M.; Jahnke, K.; Ragoss, C.; Maier, H.R. Comparative Investigation of the Biocompatibility of Various Silicon Nitride Ceramic Qualities In Vitro. *J. Mater. Sci. Mater. Med.* **2004**, *15*, 1135–1140. [[CrossRef](#)] [[PubMed](#)]
7. Gorth, D.J.; Puckett, S.; Ercan, B.; Webster, T.J.; Rahaman, M.; Bal, B.S. Decreased Bacteria Activity on Si<sub>3</sub>N<sub>4</sub> Surfaces Compared with PEEK or Titanium. *Int. J. Nanomed.* **2012**, *7*, 4829–4840.

8. Webster, T.J.; Patel, A.A.; Rahaman, M.N.; Bal, B.S. Anti-Infective and Osteointegration Properties of Silicon Nitride, Poly (Ether Ether Ketone), and Titanium Implants. *Acta Biomater.* **2012**, *8*, 4447–4454. [[CrossRef](#)] [[PubMed](#)]
9. Fischer, T.E.; Tomizawa, H. Interaction of Tribochemistry and Microfracture in the Friction and Wear of Silicon Nitride. *Wear* **1985**, *105*, 29–45. [[CrossRef](#)]
10. Tomizawa, H.; Fischer, T.E. Friction and Wear of Silicon Nitride and Silicon Carbide in Water: Hydrodynamic Lubrication at Low Sliding Speed Obtained by Tribochemical Wear. *ASLE Trans.* **1987**, *30*, 41–46. [[CrossRef](#)]
11. Ishigaki, H.; Nagata, R.; Iwasa, M. Effect of Adsorbed Water on Friction of Hot-Pressed Silicon Nitride and Silicon Carbide at Slow Speed Sliding. *Wear* **1988**, *121*, 107–116. [[CrossRef](#)]
12. Sasaki, S. The Effects of the Surrounding Atmosphere on the Friction and Wear of Alumina, Zirconia, Silicon Carbide and Silicon Nitride. *Wear* **1989**, *134*, 185–200. [[CrossRef](#)]
13. Saito, T.; Imada, Y.; Honda, F. An Analytical Observation of the Tribochemical Reaction of Silicon Nitride Sliding with Low Friction in Aqueous Solutions. *Wear* **1997**, *205*, 153–159. [[CrossRef](#)]
14. Zhou, Y.S.; Ikeuchi, K.; Ohashi, M. Comparison of the Friction Properties of Four Ceramic Materials for Joint Replacements. *Wear* **1997**, *210*, 171–177. [[CrossRef](#)]
15. Xu, J.; Kato, K. Formation of Tribochemical Layer of Ceramics Sliding in Water and its Role for Low Friction. *Wear* **2000**, *245*, 61–75. [[CrossRef](#)]
16. Satoh, T.; Sakaguchi, S.; Hirao, K.; Toriyama, M.; Kanzaki, S. Influence of Aluminum–Oxygen–Yttrium Solid Solution on the Aqueous Tribological Behavior of Silicon Nitride. *J. Am. Ceram. Soc.* **2001**, *84*, 462–464. [[CrossRef](#)]
17. Chen, M.; Kato, K.; Adachi, K. The Comparisons of Sliding Speed and Normal Load Effect on Friction Coefficients of Self-Mated  $\text{Si}_3\text{N}_4$  and  $\text{SiC}$  Under Water Lubrication. *Tribol. Int.* **2002**, *35*, 129–135. [[CrossRef](#)]
18. Maw, W.; Stevens, F.; Langford, S.C.; Dickinson, J.T. Single Asperity Tribochemical Wear of Silicon Nitride Studied by Atomic Force Microscopy. *J. Appl. Phys.* **2002**, *92*, 5103–5109. [[CrossRef](#)]
19. Jahanmir, S. Wear Transitions and Tribochemical Reactions in Ceramics. *Proc. Inst. Mech. Eng. Part J J. Eng. Tribol.* **2002**, *216*, 371–385. [[CrossRef](#)]
20. Jahanmir, S.; Ozmen, Y.; Ives, L.K. Water Lubrication of Silicon Nitride in Sliding. *Tribol. Lett.* **2004**, *17*, 409–417. [[CrossRef](#)]
21. Nakamura, N.; Hirao, K.; Yamauchi, Y. Tribological Properties of Silicon Nitride Ceramics Modified by Ion Implantation. *J. Eur. Ceram. Soc.* **2004**, *24*, 219–224. [[CrossRef](#)]
22. Amutha Rani, D.; Yoshizawa, Y.; Jones, M.I.; Hyuga, H.; Hirao, K.; Yamauchi, Y. Comparison of Tribological Behavior Between  $\alpha$ -Sialon/ $\text{Si}_3\text{N}_4$  and  $\text{Si}_3\text{N}_4$ / $\text{Si}_3\text{N}_4$  Sliding Pairs in Water Lubrication. *J. Am. Ceram. Soc.* **2005**, *88*, 1655–1658. [[CrossRef](#)]
23. Tang, Q.; Chen, J.; Liu, L. Tribological Behaviours of Carbon Fibre Reinforced PEEK Sliding on Silicon Nitride Lubricated with Water. *Wear* **2010**, *269*, 541–546. [[CrossRef](#)]
24. Ferreira, V.; Yoshimura, H.N.; Sinatora, A. Ultra-Low Friction Coefficient in Alumina–Silicon Nitride Pair Lubricated with Water. *Wear* **2012**, *296*, 656–659. [[CrossRef](#)]
25. Gee, M.G. Wear Testing and Ceramics. *Proc. Inst. Mech. Eng. Part J J. Eng. Tribol.* **1994**, *208*, 153–166. [[CrossRef](#)]
26. Dante, R.C.; Kajdas, C.K. A Review and a Fundamental Theory of Silicon Nitride Tribochemistry. *Wear* **2012**, *288*, 27–38. [[CrossRef](#)]
27. Scholes, S.C.; Unsworth, A.; Goldsmith, A.A.J. A Frictional Study of Total Hip Joint Replacements. *Phys. Med. Biol.* **2000**, *45*, 3721–3735. [[CrossRef](#)] [[PubMed](#)]
28. Cho, H.J.; Wei, W.J.; Kao, H.C.; Cheng, C.K. Wear Behavior of UHMWPE Sliding on Artificial Hip Arthroplasty Materials. *Mater. Chem. Phys.* **2004**, *88*, 9–16. [[CrossRef](#)]
29. Xiong, D.; Ge, S. Friction and Wear Properties of UHMWPE/ $\text{Al}_2\text{O}_3$  Ceramic under Different Lubricating Conditions. *Wear* **2001**, *250*, 242–245. [[CrossRef](#)]
30. Sawyer, W.G.; Argibay, N.; Burris, D.L.; Krick, B.A. Mechanistic Studies in Friction and Wear of Bulk Materials. *Annu. Rev. Mater. Res.* **2013**, *44*, 395–427. [[CrossRef](#)]
31. McKellop, H.; Clarke, I.; Markolf, K.; Amstutz, H. Friction and Wear Properties of Polymer, Metal, and Ceramic Prosthetic Joint Materials Evaluated on a Multichannel Screening Device. *J. Biomed. Mater. Res.* **1981**, *15*, 619–653. [[CrossRef](#)] [[PubMed](#)]

32. Olofsson, J.; Grehk, T.; Berling, T. Evaluation of Silicon Nitride as a Wear Resistant and Resorbable Alternative for Total Hip Joint Replacement. *Biomater* **2012**, *2*, 94–102. [[CrossRef](#)] [[PubMed](#)]
33. Mazzocchi, M.; Bellosi, A. On the Possibility of Silicon Nitride as a Ceramic for Structural Orthopaedic Implants. Part I: Processing, Microstructure, Mechanical Properties, Cytotoxicity. *J. Mater. Sci. Mater. Med.* **2008**, *19*, 2881–2887. [[CrossRef](#)] [[PubMed](#)]
34. Mazzocchi, M.; Gardini, D.; Traverso, P.L.; Faga, M.G.; Bellosi, A. On the Possibility of Silicon Nitride as a Ceramic for Structural Orthopaedic Implants. Part II: Chemical Stability and Wear Resistance in Body Environment. *J. Mater. Sci. Mater. Med.* **2008**, *19*, 2889–2901. [[CrossRef](#)] [[PubMed](#)]
35. Affatato, S.; Spinelli, M.; Zavalloni, M.; Mazzega-Fabbro, C.; Viceconti, M. Tribology and Total Hip Joint Replacement: Current Concepts in Mechanical Simulation. *Med. Eng. Phys.* **2008**, *30*, 1305–1317. [[CrossRef](#)] [[PubMed](#)]
36. Kaddick, C.; Wimmer, M.A. Hip Simulator Wear Testing According to the Newly Introduced Standard ISO 14242. *Proc. Inst. Mech. Eng. Part H J. Eng. Med.* **2001**, *215*, 429–442. [[CrossRef](#)]
37. McEntire, B.J.; Lakshminarayanan, R.; Thirugnanasambandam, P.; Seitz-Sampson, J.; Bock, R.; O'Brien, D. Processing and Characterization of Silicon Nitride Bioceramics. *Bioceram. Dev. Appl.* **2016**, *6*, 1000093. [[CrossRef](#)]
38. Taddei, P.; Affatato, S.; Fagnano, C.; Bordini, B.; Tinti, A.; Toni, A. Vibrational Spectroscopy of Ultra-High Molecular Weight Polyethylene Hip Prostheses: Influence of the Sterilisation Method on Crystallinity and Surface Oxidation. *J. Mol. Struct.* **2002**, *613*, 121–129. [[CrossRef](#)]
39. Mutter, R.; Stille, W.; Strobl, G. Transition Regions and Surface Melting in Partially Crystalline Polyethylene: A Raman Spectroscopic Study. *J. Polym. Sci. Part B Polym. Phys.* **1993**, *31*, 99–105. [[CrossRef](#)]
40. Strobl, G.R.; Hagedorn, W. Raman Spectroscopic Method for Determining the Crystallinity of Polyethylene. *J. Polym. Sci. Polym. Phys. Ed.* **1978**, *16*, 1181–1193. [[CrossRef](#)]
41. Rull, F.; Prieto, A.C.; Casado, J.M.; Sobron, F.; Edwards, H.G.M. Estimation of Crystallinity in Polyethylene by Raman Spectroscopy. *J. Raman Spectrosc.* **1993**, *24*, 545–550. [[CrossRef](#)]
42. Glotin, M.; Mandelkern, L. A Raman Spectroscopic Study of the Morphological Structure of the Polyethylenes. *Colloid Polym. Sci.* **1982**, *260*, 182–192. [[CrossRef](#)]
43. Naylor, C.C.; Meier, R.J.; Kip, B.J.; Williams, K.P.; Mason, S.M.; Conroy, N.; Gerrard, D.L. Raman Spectroscopy Employed for the Determination of the Intermediate Phase in Polyethylene. *Macromolecules* **1995**, *28*, 2969–2978. [[CrossRef](#)]
44. Taddei, P.; Di Foggia, M.; Affatato, S. Raman Characterisation of Conventional and Cross-Linked Polyethylene in Acetabular Cups Run on a Hip Joint Simulator. *J. Raman Spectrosc.* **2011**, *42*, 1344–1352. [[CrossRef](#)]
45. McKellop, H.; Lu, B.; Benya, P.; Park, S.H. Friction, Lubrication and Wear of Cobalt-Chromium Alumina and Zirconia Hip Prostheses Compared on a Joint Simulator. In *Transactions of the Orthopaedic Research Society*; Orthopaedic Research Society: Washington, DC, USA, 1992.
46. *Standard Specification for High-Purity Dense Aluminum Oxide for Medical Applications*; ASTM F603-00; Document Center Inc.: Belmont, CA, USA, 2000.
47. Grupp, T.M.; Holderied, M.; Mulliez, M.A.; Streller, R.; Jäger, M.; Blömer, W.; Utzschneider, S. Biotribology of a Vitamin E-Stabilized Polyethylene for Hip Arthroplasty—Influence of Artificial Ageing and Third-Body Particles on Wear. *Acta Biomater.* **2014**, *10*, 3068–3078. [[CrossRef](#)] [[PubMed](#)]
48. Affatato, S.; Bracco, P.; Costa, L.; Villa, T.; Quaglini, V.; Toni, A. In Vitro Wear Performance of Standard, Crosslinked, and Vitamin-E-Blended UHMWPE. *J. Biomed. Mater. Res. A* **2012**, *100*, 554–560. [[CrossRef](#)] [[PubMed](#)]
49. Galvin, A.L.; Jennings, L.M.; Tipper, J.L.; Ingham, E.; Fisher, J. Wear and Creep of Highly Crosslinked Polyethylene against Cobalt Chrome and Ceramic Femoral Heads. *Proc. Inst. Mech. Eng. Part H J. Eng. Med.* **2010**, *224*, 1175–1183. [[CrossRef](#)]
50. Al-Hajjar, M.; Jennings, L.M.; Begand, S.; Oberbach, T.; Delfosse, D.; Fisher, J. Wear of Novel Ceramic-on-Ceramic Bearings Under Adverse and Clinically Relevant Hip Simulator Conditions. *J. Biomed. Mater. Res. Part B Appl. Biomater.* **2013**, *101*, 1456–1462. [[CrossRef](#)] [[PubMed](#)]
51. Johnson, A.J.; Loving, L.; Herrera, L.; Delanois, R.E.; Wang, A.; Mont, M.A. Short-Term Wear Evaluation of Thin Acetabular Liners on 36-mm Femoral Heads. *Clin. Orthop. Relat. Res.* **2014**, *472*, 624–629. [[CrossRef](#)] [[PubMed](#)]

52. Halma, J.J.; Señaris, J.; Delfosse, D.; Lerf, R.; Oberbach, T.; van Gaalen, S.M.; de Gast, A. Edge Loading Does Not Increase Wear Rates of Ceramic-on-Ceramic and Metal-on-Polyethylene Articulations. *J. Biomed. Mater. Res. Part B Appl. Biomater.* **2014**, *102*, 1–12. [[CrossRef](#)] [[PubMed](#)]
53. Greer, K.; Chan, F.; Liao, P.; McNulty, D.; King, R. Wear of Crosslinked UHMWPE as a Function of Irradiation Dose and Crosslink Density. In Proceedings of the 48th Annual Meeting of the Orthopaedic Research Society, Dallas, TX, USA, 10–13 February 2002; Paper No. 0052; Orthopaedic Research Society Press: Rosemont, IL, USA, 2002; Volume 24.
54. Endo, M.; Tipper, J.L.; Barton, D.C.; Stone, M.H.; Ingham, E.; Fisher, J. Comparison of Wear, Wear Debris and Functional Biological Activity of Moderately Crosslinked and Non-Crosslinked Polyethylenes in Hip Prostheses. *Proc. Inst. Mech. Eng. Part H J. Eng. Med.* **2002**, *216*, 111–122. [[CrossRef](#)]
55. Galvin, A.L.; Tipper, J.L.; Jennings, L.M.; Stone, M.H.; Jin, Z.M.; Ingham, E.; Fisher, J. Wear and Biological Activity of Highly Crosslinked Polyethylene in the Hip under Low Serum Protein Concentrations. *Proc. Inst. Mech. Eng. Part H J. Eng. Med.* **2007**, *221*, 1–10. [[CrossRef](#)]
56. Smith, S.L.; Unsworth, A. A Comparison between Gravimetric and Volumetric Techniques of Wear Measurement of UHMWPE Acetabular Cups against Zirconia and Cobalt-Chromium-Molybdenum Femoral Heads in a Hip Simulator. *Proc. Inst. Mech. Eng. Part H J. Eng. Med.* **1999**, *213*, 475–483. [[CrossRef](#)]
57. Saikko, V.; Ahlroos, T.; Caloni, O.; Kera, J. Wear Simulation of Total Hip Prostheses with Polyethylene against CoCr, Alumina and Diamond-Like Carbon. *Biomaterials* **2001**, *22*, 1507–1514. [[CrossRef](#)]
58. Barbour, P.S.M.; Stone, M.H.; Fisher, J. A Hip Joint Simulator Study Using Simplified Loading and Motion Cycles Generating Physiological Wear Paths and Rates. *Proc. Inst. Mech. Eng. Part H J. Eng. Med.* **1999**, *213*, 455–467. [[CrossRef](#)]
59. Barbour, P.S.; Stone, M.H.; Fisher, J. A Hip Joint Simulator Study Using New and Physiologically Scratched Femoral Heads with Ultra-High Molecular Weight Polyethylene Acetabular Cups. *Proc. Inst. Mech. Eng. Part H J. Eng. Med.* **2000**, *214*, 569–576. [[CrossRef](#)]
60. Kaddick, C.; Pfaff, H.G. Results of Hip Simulator Testing with Various Wear Couples. In *Bioceramics in Joint Arthroplasty*, Proceedings of the 7th International BIOLOX<sup>®</sup> Symposium, Stuttgart, Germany, 15–16 March 2002; Garino, J.P., Willmann, G., Eds.; Georg Thieme Verlag Publisher: Stuttgart, Germany, 2002; pp. 16–20.
61. Okazaki, Y. Effect of Head Size on Wear Properties of Metal-on-Metal Bearings of Hip Prostheses, and Comparison with Wear Properties of Metal-on-Polyethylene Bearings using Hip Simulator. *J. Mech. Behav. Biomed. Mater.* **2014**, *31*, 152–163. [[CrossRef](#)] [[PubMed](#)]
62. Bowsher, J.G.; Clarke, I.C. Thermal Conductivity of Femoral Ball Strongly Influenced UHMWPE Wear in a Hip Simulator. In Proceedings of the Transactions of the 53rd Annual Meeting of the Orthopaedic Research Society, San Diego, CA, USA, 11–14 February 2007; Orthopaedic Research Society: San Diego, CA, USA, 2007; p. 278.
63. Zietz, C.; Fabry, C.; Middelborg, L.; Fulda, G.; Mittelmeier, W.; Bader, R. Wear Testing and Particle Characterisation of Sequentially Crosslinked Polyethylene Acetabular Liners using Different Femoral Head Sizes. *J. Mater. Sci. Mater. Med.* **2013**, *24*, 2057–2065. [[CrossRef](#)] [[PubMed](#)]
64. Masson, B.; Pandorf, T. Wear Behavior of AMC Ceramics on PE in Hip Prostheses. *J. Bone Jt. Surg. Br.* **2011**, *93*, 221.
65. Lee, R.; Essner, A.; Wang, A.; Jaffe, W.L. Scratch and Wear Performance of Prosthetic Femoral Head Components against Crosslinked UHMWPE Sockets. *Wear* **2009**, *267*, 1915–1921. [[CrossRef](#)]
66. Liao, Y.-S.; Greer, K.; Alberts, A. Effect of Head Material and Roughness on the Wear of 7.5 MRad Crosslinked-Remelted UHMWPE Acetabular Inserts. In Proceedings of the 54th Annual Meeting of the Orthopaedic Research Society, San Francisco, CA, USA, 2–5 March 2008; Orthopaedic Research Society Press: Rosemont, IL, USA, 2008; p. 1901.
67. Bigsby, R.J.A.; Hardaker, C.S.; Fisher, J. Wear of Ultra-High Molecular Weight Polyethylene Acetabular Cups in a Physiological Hip Joint Simulator in the Anatomical Position using Bovine Serum as a Lubricant. *Proc. Inst. Mech. Eng. Part H J. Eng. Med.* **1997**, *211*, 265–269. [[CrossRef](#)]
68. Williams, S.; Butterfield, M.; Stewart, T.; Ingham, E.; Stone, M.; Fisher, J. Wear and Deformation of Ceramic-on-Polyethylene Total Hip Replacements with Joint Laxity and Swing Phase Microseparation. *Proc. Inst. Mech. Eng. Part H J. Eng. Med.* **2003**, *217*, 147–153. [[CrossRef](#)]

69. Roy, M.E.; Whiteside, L.A.; Magill, M.E.; Katerberg, B.J. Reduced Wear of Cross-Linked UHMWPE Using Magnesia-Stabilized Zirconia Femoral Heads in a Hip Simulator. *Clin. Orthop. Relat. Res.* **2011**, *469*, 2337–2345. [[CrossRef](#)] [[PubMed](#)]
70. Puppulin, L.; Kumakura, T.; Yamamoto, K.; Pezzotti, G. Structural Profile of Ultra-High Molecular Weight Polyethylene in Acetabular Cups Worn on Hip Simulators Characterized by Confocal Raman Spectroscopy. *J. Orthop. Res.* **2011**, *29*, 893–899. [[CrossRef](#)] [[PubMed](#)]
71. Oral, E.; Christensen, S.D.; Malhi, A.S.; Wannomae, K.K.; Muratoglu, O.K. Wear Resistance and Mechanical Properties of Highly Cross-Linked, Ultrahigh-Molecular Weight Polyethylene Doped with Vitamin E. *J. Arthroplast.* **2006**, *21*, 580–591. [[CrossRef](#)] [[PubMed](#)]
72. Affatato, S.; Frigo, M.; Toni, A. An In Vitro Investigation of Diamond-Like Carbon as a Femoral Head Coating. *J. Biomed. Materials Res.* **2000**, *53*, 221–226. [[CrossRef](#)]
73. Billi, F.; Benya, P.; Kavanaugh, A.; Adams, J.; McKellop, H.; Ebramzadeh, E. An Accurate and Extremely Sensitive Method to Separate, Display, and Characterize Wear Debris: Part 2: Metal and Ceramic Particles. *Clin. Orthop. Relat. Res.* **2012**, *470*, 339–350. [[CrossRef](#)] [[PubMed](#)]
74. Davidson, J.A.; Poggie, R.A.; Mishra, A.K. Abrasive Wear of Ceramic, Metal, and UHMWPE Bearing Surfaces from Third-Body Bone, PMMA Bone Cement, and Titanium Debris. *Biomed. Mater. Eng.* **1994**, *4*, 213–229. [[PubMed](#)]
75. Garvin, K.L.; Hartman, C.W.; Mangla, J.; Murdoch, N.; Martell, J.M. Wear Analysis in THA Utilizing Oxidized Zirconium and Crosslinked Polyethylene. *Clin. Orthop. Relat. Res.* **2009**, *467*, 141–145. [[CrossRef](#)] [[PubMed](#)]
76. Saikko, V.; Ahlroos, T. Type of Motion and Lubricant in Wear Simulation of Polyethylene Acetabular Cup. *Proc. Inst. Mech. Eng. Part H J. Eng. Med.* **1999**, *213*, 301–310. [[CrossRef](#)]
77. Affatato, S.; Bordini, B.; Fagnano, C.; Taddei, P.; Tinti, A.; Toni, A. Effects of the Sterilisation Method on the Wear of UHMWPE Acetabular Cups Tested in a Hip Joint Simulator. *Biomaterials* **2002**, *23*, 1439–1446. [[CrossRef](#)]
78. Smith, S.L.; Unsworth, A. A Five-Station Hip Joint Simulator. *Proc. Inst. Mech. Eng. Part H J. Eng. Med.* **2001**, *215*, 61–64. [[CrossRef](#)]
79. Fisher, J.; Galvin, A.; Tipper, J.; Stewart, T.; Stone, M.; Ingham, E. Comparison of the Functional Biological Activity and Osteolytic Potential of Ceramic and Cross Linked Polyethylene Bearings in the Hip. In *Bioceramics and Alternative Bearings in Joint Arthroplasty*, Proceedings of the 10th BIOLOX<sup>®</sup> Symposium, Washington, DC, USA, 10–11 June 2005; D'Antonio, J.A., Dietrich, M., Eds.; Steinkopff Verlag: Darmstadt, Germany, 2005; pp. 21–24.
80. Jedenmalm, A.; Affatato, S.; Taddei, P.; Leardini, W.; Gedde, U.W.; Fagnano, C.; Viceconti, M. Effect of Head Surface Roughness and Sterilization on Wear of UHMWPE Acetabular Cups. *J. Biomed. Mater. Res. A* **2009**, *90*, 1032–1042. [[CrossRef](#)] [[PubMed](#)]
81. Smith, S.L.; Unsworth, A. Simplified Motion and Loading Compared to Physiological Motion and Loading in a Hip Joint Simulator. *Proc. Inst. Mech. Eng. Part H J. Eng. Med.* **2000**, *214*, 233–238. [[CrossRef](#)]
82. Affatato, S.; Zavalloni, M.; Spinelli, M.; Costa, L.; Bracco, P.; Viceconti, M. Long-Term In Vitro Wear Performance of an Innovative Thermo-Compressed Cross-Linked Polyethylene. *Tribol. Int.* **2010**, *43*, 22–28. [[CrossRef](#)]
83. Clarke, I.C.; Gustafson, A.; Jung, H.; Fujisawa, A. Hip-Simulator Ranking of Polyethylene Wear: Comparisons between Ceramic Heads of Different Sizes. *Acta Orthop. Scand.* **1996**, *67*, 128–132. [[CrossRef](#)] [[PubMed](#)]
84. Ezzet, K.A.; Hermida, J.C.; Steklov, N.; D'Lima, D.D. Wear of Polyethylene against Oxidized Zirconium Femoral Components. Effect of Aggressive Kinematic Conditions and Malalignment in Total Knee Arthroplasty. *J. Arthroplast.* **2012**, *27*, 116–121. [[CrossRef](#)] [[PubMed](#)]
85. Takahashi, Y.; Masaoka, T.; Yamamoto, K.; Shishido, T.; Tateiwa, T.; Kubo, K.; Pezzotti, G. Vitamin-E Blended and Infused Highly Cross-Linked Polyethylene for Total Hip Arthroplasty: A Comparison of Three-Dimensional Crystalline Morphology and Strain Recovery Behavior. *J. Mech. Behav. Biomed. Mater.* **2014**, *36*, 59–70. [[CrossRef](#)]
86. Affatato, S.; Freccero, N.; Taddei, P. The Biomaterials Challenge: A Comparison of Polyethylene Wear Using a Hip Joint Simulator. *J. Mech. Behav. Biomed. Mater.* **2016**, *53*, 40–48. [[CrossRef](#)]

87. Tipper, J.L.; Galvin, A.L.; Williams, S.; McEwen, H.M.J.; Stone, M.H.; Ingham, E.; Fisher, J. Isolation and Characterization of UHMWPE Wear Particles Down to Ten Nanometers in Size from In Vitro Hip and Knee Joint Simulators. *J. Biomed. Mater. Res.* **2006**, *78A*, 473–480.
88. Shen, F.-W.; Lu, Z.; McKellop, H.A. Wear versus Thickness and other Features of 5-Mrad Crosslinked UHMWPE Acetabular Liners. *Clin. Orthop. Relat. Res.* **2011**, *469*, 395–404. [[CrossRef](#)]
89. Sorimachi, T.; Clarke, I.C.; Williams, P.A.; Gustafson, A.; Yamamoto, K. Third-Body Abrasive Wear Challenge of 32 mm Conventional and 44 mm Highly Crosslinked Polyethylene Liners in a Hip Simulator Model. *Proc. Inst. Mech. Eng. Part H J. Eng. Med.* **2009**, *223*, 607–623. [[CrossRef](#)]
90. Herrera, L.; Lee, R.; Essner, A.; Longaray, J.; Wang, A.; Dumbleton, J.H.; Lovell, T. Hip Simulator Evaluation of the Effect of Femoral Head Size and Liner Thickness on the Wear of Sequentially Crosslinked Acetabular Liners. In Proceedings of the 53rd Annual Meeting of the Orthopaedic Research Society, San Diego, CA, USA, 11–14 February 2007; Orthopaedic Research Society Press: Rosemont, IL, USA, 2007; p. 181.
91. Kubo, K.; Clarke, I.C.; Sorimachi, T.; Williams, P.A.; Donaldson, T.K.; Yamamoto, K. Aggressive 3rd-Body Wear Challenge to Highly Crosslinked Polyethylene: A Hip Simulator Model. *Wear* **2009**, *267*, 734–742. [[CrossRef](#)]
92. Galvin, A.; Brockett, C.; Williams, S. Comparison of Wear of Ultra-High Molecular Weight Polyethylene Acetabular Cups against Surface-Engineered Femoral Heads. *Proc. Inst. Mech. Eng. Part H J. Eng. Med.* **2008**, *222*, 1073–1080. [[CrossRef](#)]
93. De Villiers, D.; Traynor, A.; Collins, S.N.; Banfield, S.; Housden, J.; Shelton, J.C. Chromium Nitride Coating for Large Diameter Metal-on-Polyethylene Hip Bearings Under Extreme Adverse Hip Simulator Conditions. *Wear* **2015**, *328–329*, 363–368. [[CrossRef](#)]
94. Affatato, S.; Zavalloni, M.; Taddei, P.; Di Foggia, M.; Fagnano, C.; Viceconti, M. Comparative Study on the Wear Behaviour of Different Conventional and Cross-Linked Polyethylenes for Total Hip Replacement. *Tribol. Int.* **2008**, *41*, 813–822. [[CrossRef](#)]
95. Estok, D.M.; Burroughs, B.R.; Muratoglu, O.K.; Harris, W.H. Comparison of Hip Simulator Wear of 2 Different Highly Cross-Linked Ultra High Molecular Weight Polyethylene Acetabular Components Using both 32- and 38-mm Femoral Heads. *J. Arthroplast.* **2007**, *22*, 581–589. [[CrossRef](#)]
96. Shishido, T.; Clarke, I.C.; Williams, P.; Boehler, M.; Asano, T.; Shoji, H.; Masaoka, T.; Yamamoto, K.; Imakiire, A. Clinical and Simulator Wear Study of Alumina Ceramic THR to 17 Years and Beyond. *J. Biomed. Mater. Res. B Appl. Biomater.* **2003**, *67*, 638–647. [[CrossRef](#)] [[PubMed](#)]
97. Oonishi, H.; Clarke, I.C.; Williams, P.A.; Shishido, T.; Gustafson, A. Characterization of Steady-State Wear in All-Alumina THR to 20 MC. *Key Eng. Mater.* **2001**, *218–220*, 587–590. [[CrossRef](#)]
98. Clarke, I.C.; Lazennec, J.Y.; Smith, E.J.; Sugano, N.; McEntire, B.J.; Pezzotti, G. Ceramic-on-Ceramic Bearings: Simulator Wear Compared to Clinical Retrieval Data. In *Material for Total Joint Arthroplasty—Biotribology of Potential Bearings*; Sonntag, R., Kretzer, J.P., Eds.; Imperial College Press: London, UK, 2015; pp. 85–131.
99. Clarke, I.C.; Green, D.D.; Williams, P.S.; Kubo, K.; Pezzotti, G.; Lombardi, A.; Turnbull, A.; Donaldson, T.K. Hip-Simulator Wear Studies of an Alumina-Matrix Composite (AMC) Ceramic Compared to Retrieval Studies of AMC Balls with 1–7 Years Follow-Up. *Wear* **2009**, *267*, 702–709. [[CrossRef](#)]
100. Bracco, P.; Brach del Prever, E.M.; Cannas, M.; Luda, M.P.; Costa, L. Oxidation Behaviour in Prosthetic UHMWPE Components Sterilised with High Energy Radiation in a Low-Oxygen Environment. *Polym. Degrad. Stab.* **2006**, *91*, 2030–2038. [[CrossRef](#)]
101. Bracco, P.; Brunella, V.; Luda, M.P.; Brach del Prever, E.M.; Zanetti, M.; Costa, L. Oxidation Behaviour in Prosthetic UHMWPE Components Sterilised with High-Energy Radiation in the Presence of Oxygen. *Polym. Degrad. Stab.* **2006**, *91*, 3057–3064. [[CrossRef](#)]
102. Costa, L.; Luda, M.P.; Trossarelli, L. Ultra High Molecular Weight Polyethylene—II. Thermal- and Photo-Oxidation. *Polym. Degrad. Stab.* **1997**, *58*, 41–54. [[CrossRef](#)]
103. Wannomae, K.K.; Bhattacharyya, S.; Freiberg, A.; Estok, D.; Harris, W.H.; Muratoglu, O. In Vivo Oxidation of Retrieved Cross-Linked Ultra-High-Molecular-Weight Polyethylene Acetabular Components with Residual Free Radicals. *J. Arthroplast.* **2006**, *21*, 1005–1011. [[CrossRef](#)] [[PubMed](#)]
104. Bhateja, S.K.; Andrews, E.H.; Yarbrough, S.M. Radiation Induced Crystallinity Changes in Linear Polyethylenes: Long Term Aging Effects. *Polym. J.* **1989**, *21*, 739–750. [[CrossRef](#)]
105. Premnath, V.; Harris, W.H.; Jasty, M.; Merrill, E.W. Gamma Sterilization of UHMWPE Articular Implants: An Analysis of the Oxidation Problem. *Biomaterials* **1996**, *17*, 1741–1753. [[CrossRef](#)]

106. Yeom, B.; Yu, Y.-J.; McKellop, H.A.; Salovey, R. Profile of Oxidation in Irradiated Polyethylene. *J. Polym. Sci. Part A Polym. Chem.* **1998**, *36*, 329–339. [[CrossRef](#)]
107. Medel, F.J.; Rimnac, C.M.; Kurtz, S.M. On the Assessment of Oxidative and Microstructural Changes after In Vivo Degradation of Historical UHMWPE Knee Components by Means of Vibrational Spectroscopies and Nanoindentation spectroscopies and nanoindentation. *J. Biomed. Mater. Res.* **2009**, *89A*, 530–538. [[CrossRef](#)] [[PubMed](#)]
108. Blanchet, T.A.; Burroughs, B.R. Numerical Oxidation Model for Gamma Radiation-Sterilized UHMWPE: Consideration of Dose-Depth Profile. *J. Biomed. Mater. Res.* **2001**, *58*, 684–693. [[CrossRef](#)] [[PubMed](#)]
109. Pezzotti, G. Bioceramics for Hip Joints: The Physical Chemistry Viewpoint. *Materials (Basel)* **2014**, *7*, 4367–4410. [[CrossRef](#)]
110. Pezzotti, G.; Bal, B.S.; Casagrande, E.; Sugano, N.; McEntire, B.J.; Zhu, W.; Puppulin, L. On the Molecular Interaction between Ceramic Femoral Heads and Polyethylene Liners in Artificial Hip Joints: II. Molecular Scale Phenomena. 2016, in press.
111. Liu, F.; Fisher, J.; Jin, Z. Effect of Motion Inputs on the Wear Prediction of Artificial Hip Joints. *Tribol. Int.* **2013**, *63*, 105–114. [[CrossRef](#)] [[PubMed](#)]
112. Zietz, C.; Fabry, C.; Reinders, J.; Dammer, R.; Kretzer, J.P.; Bader, R.; Sonntag, R. Wear Testing of Total Hip Replacements Under Severe Conditions. *Expert Rev. Med. Devices* **2015**, *12*, 393–410. [[CrossRef](#)] [[PubMed](#)]
113. Oliveira, A.L.L.; Trigo, F.C.; Martins, F.P.R. Quantitative Evaluation of Parameters Used in Wear Testing Simulators of Total Hip Arthroplasty Components. *Wear* **2014**, *313*, 1–10. [[CrossRef](#)]
114. Maskiewicz, V.K.; Williams, P.A.; Prates, S.J.; Bowsher, J.G.; Clarke, I.C. Characterization of Protein Degradation in Serum-Based Lubricants during Simulation Wear Testing of Metal-on-Metal Hip Prostheses. *J. Biomed. Mater. Res. Part B Appl. Biomater.* **2010**, *94B*, 429–440. [[CrossRef](#)] [[PubMed](#)]
115. Myant, C.; Underwood, R.; Fan, J.; Cann, P.M. Lubrication of Metal-on-Metal Hip Joints: The Effect of Protein Content and Load on Film Formation and Wear. *J. Mech. Behav. Biomed. Mater.* **2012**, *6*, 30–40. [[CrossRef](#)] [[PubMed](#)]
116. Sun, D.; Wharton, J.A.; Wood, R.J.W. The Effects of Proteins and pH on Tribo-Corrosion Performance of Cast CoCrMo: A Combined Electrochemical and Tribological Study. *Tribol. Surfaces Interfaces* **2008**, *2*, 150–160. [[CrossRef](#)]
117. Vrbka, M.; Křupka, I.; Hartl, M.; Návrát, T.; Gallo, J.; Galandáková, A. In Situ Measurements of Thin Films in Bovine Serum Lubricated Contacts Using Optical Interferometry. *Proc. Inst. Mech. Eng. Part H J. Eng. Med.* **2014**, *228*, 149–158. [[CrossRef](#)] [[PubMed](#)]
118. Lu, Z.; McKellop, H. Frictional Heating of Bearing Materials Tested in a Hip Joint Wear Simulator. *Proc. Inst. Mech. Eng. Part H J. Eng. Med.* **1997**, *211*, 101–108. [[CrossRef](#)]
119. Good, V.; Clarke, I.C.; Gustafson, A.; Braham, A.; Downs, B.; Sorensen, K.; Anissian, L. Dose Response of Protein Concentration to Wear in PTFE and UHMWPE. In Proceedings of the 45th Annual Meeting of the Orthopaedic Research Society, Anaheim, CA, USA, 1–4 February 1999; Orthopaedic Research Society: Anaheim, CA, USA, 1999; p. 839.
120. Liao, Y.-S.; Benya, P.D.; McKellop, H.A. Effect of Protein Lubrication on the Wear Properties of Materials for Prosthetic Joints. *J. Biomed. Mater. Res.* **1999**, *48*, 465–473. [[CrossRef](#)]
121. Clarke, I.C.; Gustafson, A. Clinical and Hip Simulator Comparisons of Ceramic-on-Polyethylene and Metal-on-Polyethylene Wear. *Clin. Orthop. Relat. Res.* **2000**, *379*, 34–40. [[CrossRef](#)] [[PubMed](#)]
122. Bell, J.; Tipper, J.L.; Ingham, E.; Stone, M.H.; Fisher, J. The Influence of Phospholipid Concentration in Protein-Containing Lubricants on the Wear of Ultra-High Molecular Weight Polyethylene in Artificial Hip Joints. *Proc. Inst. Mech. Eng. Part H J. Eng. Med.* **2001**, *215*, 259–263. [[CrossRef](#)]
123. Wang, A.; Essner, A.; Schmidig, G. The Effects of Lubricant Composition on In Vitro Wear Testing of Polymeric Acetabular Components. *J. Biomed. Mater. Res. B Appl. Biomater.* **2004**, *68*, 45–52. [[CrossRef](#)] [[PubMed](#)]
124. Tsai, S.; Salehi, A.; Aldinger, P.; Hunter, G. Heat Generation and Dissipation Behavior of Various Orthopaedic Bearing Materials. *Key Eng. Mater.* **2006**, *309–311*, 1291–1294. [[CrossRef](#)]
125. Guenther, L.E.; Turgeon, T.R.; Bohm, E.R.; Brandt, J.-M. The Biochemical Characteristics of Wear Testing Lubricants Affect Polyethylene Wear in Orthopaedic Pin-on-Disc Testing. *Proc. Inst. Mech. Eng. Part H J. Eng. Med.* **2015**, *229*, 77–90. [[CrossRef](#)] [[PubMed](#)]

126. Myshkin, N.K.; Petrokovets, M.I.; Kovalev, A.V. Tribology of Polymers: Adhesion, Friction, Wear, and Mass-Transfer. *Tribol. Int.* **2005**, *38*, 910–921. [[CrossRef](#)]
127. Galetz, M.C.; Seiferth, S.H.; Theile, B.; Glatzel, U. Potential for Adhesive Wear in Friction Couples of UHMWPE Running Against Oxidized Zirconium, Titanium Nitride Coatings, and Cobalt-Chromium Alloys. *J. Biomed. Mater. Res. B Appl. Biomater.* **2010**, *93*, 468–475. [[CrossRef](#)] [[PubMed](#)]
128. Wang, A.; Essner, A.; Polineni, V.K.; Stark, C.; Dumbleton, J.H. Lubrication and Wear of Ultra-High Molecular Weight Polyethylene in Total Joint Replacements. *Tribol. Int.* **1998**, *31*, 17–33. [[CrossRef](#)]
129. Lee, S.K.; Lawn, B.R. Contact Fatigue in Silicon Nitride. *J. Am. Ceram. Soc.* **1999**, *82*, 1281–1288. [[CrossRef](#)]
130. Lawn, B.R.; Lee, S.K.; Peterson, I.M.; Wuttiphon, S. Model of Strength Degradation from Hertzian Contact Damage in Tough Ceramics. *J. Am. Ceram. Soc.* **1998**, *81*, 1509–1520. [[CrossRef](#)]
131. Lee, K.S.; Jung, Y.; Peterson, I.M.; Lawn, B.R.; Kim, D.; Lee, S.K. Model for Cyclic Fatigue of Quasi-Plastic Ceramics in Contact with Spheres. *J. Am. Ceram. Soc.* **2000**, *83*, 2255–2262. [[CrossRef](#)]
132. Zhu, W.; Puppulin, L.; Leto, A.; Takahashi, Y.; Sugano, N.; Pezzotti, G. In Situ Measurements of Local Temperature and Contact Stress Magnitude during Wear of Ceramic-on-Ceramic Hip Joints. *J. Mech. Behav. Biomed. Mater.* **2014**, *31*, 68–76. [[CrossRef](#)] [[PubMed](#)]
133. Sonntag, R.; Reinders, J.; Rieger, J.S.; Heitzmann, D.W.W.; Kretzer, J.P. Hard-on-Hard Lubrication in the Artificial Hip Under Dynamic Loading Conditions. *PLoS ONE* **2013**, *8*, e71622. [[CrossRef](#)] [[PubMed](#)]
134. Bergstrom, L.; Pugh, R.J. Interfacial Characterization of Silicon Nitride Powders. *J. Am. Ceram. Soc.* **1989**, *72*, 103–109. [[CrossRef](#)]
135. NIST-JANAF Thermochemical Tables. Available online: <http://kinetics.nist.gov/janaf/> (accessed on 12 October 2016).
136. Mizutani, T.; Nagase, H.; Fujiwara, N.; Ogoshi, H. Silicic Acid Polymerization Catalyzed by Amines and Polyamines. *Bull. Chem. Soc. Jpn.* **1998**, *71*, 2017–2022. [[CrossRef](#)]
137. Sui, X.; Wang, B.; Liu, Y.; Wu, H.; Li, Q.; Zhang, Q. Study on Microstructure of Polysilicic Acid in High Salinity. *J. Appl. Sci. Eng. Innov.* **2014**, *1*, 44–48.
138. Zhu, W.; McEntire, B.J.; Enomoto, Y.; Boffelli, M.; Pezzotti, G. Point-Defect Populations as Induced by Cation/Anion Substitution in  $\beta$ -Si<sub>3</sub>N<sub>4</sub> Lattice—A Cathodoluminescence Study. *J. Phys. Chem. C* **2015**, *119*, 3279–3287. [[CrossRef](#)]
139. Gates, R.S.; Hsu, M.; Klaus, E.E. Tribochemical Mechanism of Alumina with Water. *Tribol. Trans.* **2008**, *32*, 357–363. [[CrossRef](#)]
140. Fischer, T.E.; Zhu, Z.; Kim, H.; Shin, D.S. Genesis and Role of Wear Debris in Sliding Wear of Ceramics. *Wear* **2000**, *245*, 53–60. [[CrossRef](#)]
141. Brockett, C.; Williams, S.; Jin, Z.; Isaac, G.; Fisher, J. Friction of Total Hip Replacements with Different Bearings and Loading Conditions. *J. Biomed. Mater. Res. Part B Appl. Biomater.* **2006**, *81B*, 508–515. [[CrossRef](#)] [[PubMed](#)]
142. Mattei, L.; Di Puccio, F.; Piccigallo, B.; Ciulli, E. Lubrication and Wear Modelling of Artificial Hip Joints: A Review. *Tribol. Int.* **2011**, *44*, 532–549. [[CrossRef](#)]
143. Iliiev, C. Wear of Water Lubricated Silicon Nitride in Ball on Disc Test. *Tribol. Mater. Surfaces Interfaces* **2010**, *4*, 15–25. [[CrossRef](#)]
144. Heshmat, H.; Jahanmir, S. Tribological Behavior of Ceramics at High Sliding Speeds in Steam. *Tribol. Lett.* **2004**, *17*, 359–366. [[CrossRef](#)]
145. Cheong, Y.S.; Mukundhan, P.; Du, H.H.; Withrow, S.P. Improved Oxidation Resistance of Silicon Nitride by Aluminum Implantation: I, Kinetics and Oxide Characteristics. *J. Am. Ceram. Soc.* **2000**, *83*, 154–160. [[CrossRef](#)]
146. Cheong, Y.S.; Mukundhan, P.; Du, H.H.; Withrow, S.P. Improved Oxidation Resistance of Silicon Nitride by Aluminum Implantation: II, Analysis and Optimization. *J. Am. Ceram. Soc.* **2000**, *83*, 161–165. [[CrossRef](#)]
147. Mukundhan, P.; Du, H.H.; Withrow, S.P. Oxidation Studies of Aluminum-Implanted NBD 200 Silicon Nitride. *J. Am. Ceram. Soc.* **2002**, *85*, 865–872. [[CrossRef](#)]
148. McEntire, B.; Lakshminarayanan, R. Coated Implants and Related Methods. U.S. Patent 9,051,639, 9 June 2015.
149. Shankar, S.; Prakash, L.; Kalayarasan, M. Finite Element Analysis of Different Contact Bearing Couples for Human Hip Prosthesis. *Int. J. Biomed. Eng. Technol.* **2013**, *11*, 66–80. [[CrossRef](#)]

150. Hodaei, M.; Farhang, K.; Maani, N. A Contact Model for Establishment of Hip Joint Implant Wear Metrics. *J. Biomed. Sci. Eng.* **2014**, *7*, 228–242. [[CrossRef](#)]
151. Shankar, S.; Nithyaprakash, R. Wear Prediction on Silicon Nitride Bearing Couple in Human Hip Prosthesis using Finite Element Concepts. *Proc. Inst. Mech. Eng. Part J. J. Tribol.* **2014**, *228*, 717–724. [[CrossRef](#)]
152. Glyn-Jones, S.; Thomas, G.E.R.; Garfjeld-Roberts, P.; Gundle, R.; Taylor, A.; McLardy-Smith, P.; Murray, D.W. Highly Crosslinked Polyethylene in Total Hip Arthroplasty Decreases Long-term Wear: A Double-blind Randomized Trial. *Clin. Orthop. Relat. Res.* **2014**, *473*, 432–438. [[CrossRef](#)] [[PubMed](#)]
153. Sato, T.; Nakashima, Y.; Akiyama, M.; Yamamoto, T.; Mawatari, T.; Itokawa, T.; Ohishi, M.; Motomura, G.; Hirata, M.; Iwamoto, Y. Comparison of Polyethylene Wear between Highly Crosslinked and Annealed UHMWPE and Conventional UHMWPE Against Ceramic Heads in Total Hip Arthroplasty. *Key Eng. Mater.* **2013**, *529–530*, 279–284. [[CrossRef](#)]
154. Kim, Y.-H.; Park, J.-W.; Kulkarni, S.S.; Kim, Y.-H. A Randomised Prospective Evaluation of Ceramic-on-Ceramic and Ceramic-on-Highly Cross-Linked Polyethylene Bearings in the Same Patients with Primary Cementless Total Hip Arthroplasty. *Int. Orthop.* **2013**, *37*, 2131–2137. [[CrossRef](#)] [[PubMed](#)]
155. Topolovec, M.; Milošev, I. A Comparative Study of Four Bearing Couples of the Same Acetabular and Femoral Component: A Mean Follow-Up of 11.5 Years. *J. Arthroplast.* **2014**, *29*, 176–180. [[CrossRef](#)] [[PubMed](#)]
156. Pezzotti, G.; Yamamoto, K. Artificial Hip Joints: The Biomaterials Challenge. *J. Mech. Behav. Biomed. Mater.* **2014**, *31*, 3–20. [[CrossRef](#)] [[PubMed](#)]
157. Moro, T.; Kyomoto, M.; Ishihara, K.; Saiga, K.; Hashimoto, M.; Tanaka, S.; Ito, H.; Tanaka, T.; Oshima, H.; Kawaguchi, H.; et al. Grafting of Poly(2-methacryloyloxyethyl phosphorylcholine) on Polyethylene Liner in Artificial Hip Joints Reduces Production of Wear Particles. *J. Mech. Behav. Biomed. Mater.* **2014**, *31*, 100–106. [[CrossRef](#)] [[PubMed](#)]
158. Takatori, Y.; Moro, T.; Ishihara, K.; Kamogawa, M.; Oda, H.; Umeyama, T.; Kim, Y.T.; Ito, H.; Kyomoto, M.; Tanaka, T.; et al. Clinical and Radiographic Outcomes of Total Hip Replacement with Poly(2-methacryloyloxyethyl phosphorylcholine)—Grafted Highly Cross-Linked Polyethylene Liners: Three-Year Results of a Prospective Consecutive Series. *Mod. Rheumatol.* **2015**, *25*, 286–291. [[CrossRef](#)] [[PubMed](#)]



© 2016 by the authors; licensee MDPI, Basel, Switzerland. This article is an open access article distributed under the terms and conditions of the Creative Commons Attribution (CC-BY) license (<http://creativecommons.org/licenses/by/4.0/>).